Frontiers in Scientific Research and Technology

Online ISSN: 2682-2970
Print ISSN: 2682-2962
http://fsrt.journals.ekb.eg

FSRT J 11 (2025) 78 - 100 10.21608/fsrt.2025.381077.1162

Fluorescent Sensors for Heavy Metal Detection: Techniques, Applications, and Environmental Impact: A Review

Rasha M. Kamel*, Sahar S. El-Sakka, Maram M. A. Abbas, M. H. A. Soliman

Suez University, Faculty of Science, Chemistry Department, 43518 Suez, Egypt

ARTICLE INFO

Article history:
Received 2 May 2025
Received in revised form 8 June 2025
Accepted 10 June 2025
Available online 10 June 2025

Keywords
Detection,
Fluorescence,
Sensor,
Fluorophore,
Pollution

ABSTRACT

Small organic molecules have emerged as powerful tools in the detection of environmental pollutants due to their ability to selectively interact with target substances. By inducing measurable changes in properties such as fluorescence, color, or electrical conductivity upon binding, these molecules enable the development of highly sensitive and specific sensors for a wide range of contaminants—including heavy metals, pesticides, and industrial chemicals—even in complex matrices. Their key advantages include high selectivity, which allows for precise recognition of target pollutants; exceptional sensitivity, where even trace-level interactions produce detectable signals; and remarkable versatility, enabling adaptation to diverse analytes. Additionally, their ease of use and cost-effectiveness make them well-suited for on-site and real-time monitoring applications. Small organic molecules are particularly valuable in fluorescent sensing platforms, where pollutant binding leads to distinct changes in fluorescence emission. These systems offer rapid, low-cost, and reliable detection suitable for field use and personal health monitoring. Compared to conventional analytical techniques, small molecule-based sensors are easier to fabricate and operate, offering a practical alternative for widespread environmental monitoring. Looking ahead, ongoing research focuses on enhancing sensor performance, lowering detection limits, broadening the spectrum of detectable pollutants, and integrating these sensors into portable, user-friendly devices. Such advances hold significant promise for improving environmental safety and public health.

1. Introduction

The accumulation of heavy metals (HMs) has become a major environmental and public health issue due to their persistent nature and toxicity. Both natural sources (such as volcanic eruptions and soil erosion) and human activities (such as industrialization, mining, agriculture, and urbanization) contribute to heavy metal pollution. However, the 20th-century industrial boom has drastically increased human exposure to such as lead (Pb), chromium (Cr), cadmium (Cd), arsenic (As), and mercury (Hg). Heavy metals enter the environment through industrial emissions, vehicle exhaust, improper waste disposal, and agricultural runoff. They contaminate air, water, and soil, leading to bioaccumulation in plants, animals, and humans. Once inside the body, heavy metals can cause acute or chronic poisoning, interfering with enzymatic functions and releasing oxygen species that are reactive (ROS) to induce oxidative stress. These processes lead to organ damage, neurological disorders, cardiovascular diseases, and increased cancer risk. The growing environmental pollution crisis highlights the urgent need for mitigation strategies to limit human and ecological exposure to heavy metals [1-3].

* Corresponding author at Suez University

E-mail addresses: rasha.abdalla@suezuniv.edu.eg (Rasha M. Kamel)

1.1 Heavy Metals and Their Role in Environmental Pollution

Heavy metals are one of the most hazardous pollutants, primarily originating from human activities such as industrial operations, mining, petroleum extraction, and the excessive use of fertilizers and pesticides. These metals accumulate in soil and water, leading to long-term environmental contamination. Urban and industrial pollution, particularly from vehicle emissions, further exacerbates heavy metal exposure, negatively impacting plant growth, crop yield, and biodiversity.

Toxic metals such as arsenic, chromium, lead, and cadmium pose severe health risks due to their bio-accumulative nature. They enter the human body through contaminated food, water, air, or direct skin contact, leading to systemic toxicity and chronic illnesses. The persistence of heavy metals in the environment highlights the need for sustainable pollution management strategies, including phytoremediation and eco-friendly remediation technologies [4-6].

1.2 Industrialization, Urbanization, and Their Contribution to Pollution

The rapid expansion of industrial and urban activities has significantly increased heavy metal pollution. Factories,

transportation systems, and chemical-intensive agricultural practices have led to widespread contamination of air, water, and soil. The growing demand for energy and resources further intensifies pollution levels, making urban and industrial areas hotspots for environmental contamination.

While natural sources like volcanic activity and wildfires contribute to heavy metal pollution, human activities remain the dominant factor. Industrial waste discharge, untreated sewage, and improper hazardous waste disposal exacerbate the problem. Water bodies, agricultural soils, and urban environments are increasingly contaminated with persistent heavy metals, posing a direct threat to human and ecological health [7-9].

1.3 Health Risks and Toxic Effects of Heavy Metals

Heavy metal exposure leads to a range of health complications, from acute toxicity to chronic diseases. These metals disrupt cellular functions, induce oxidative stress, and inhibit essential enzymes, leading to severe health consequences. The following are the main ways that humans get exposed:

- Consuming tainted food and water
- Exposure to airborne contaminants
- Dermal absorption through direct contact with contaminated surfaces

While some metals, like zinc, play crucial biological roles as enzyme cofactors and antioxidants, excessive exposure to toxic metals like lead, cadmium, and arsenic results in neurotoxicity, kidney damage, cardiovascular disorders, and cancer. Heavy metals are also implicated in metabolic disorders such as diabetes, infertility, and immune dysfunction [10-12].

2. Heavy Metals in Biological Systems: Roles and Toxicity

2.1 Essential vs. Non-Essential Metals

Metals play a dual role in biological systems—some are essential for life, while others are purely toxic. Essential metals such as manganese (Mn), iron (Fe), copper (Cu), and zinc (Zn)

support metabolic processes and act as cofactors in enzymatic reactions. Nearly 50% of all enzymes require a metal cofactor to function effectively. However, even these beneficial metals can become harmful if present in excess.

Non-essential metals such as arsenic, cadmium, mercury, nickel, and vanadium have no biological benefits and are hazardous even in trace amounts. These toxic metals interfere with metabolic pathways, disrupt protein functions, and contribute to severe health conditions. The growing exposure to both essential and non-essential metals is a global concern, as they are linked to chronic diseases, including cancer and metabolic disorders [13-14].

2.2 Heavy Metals and Cancer Development

Heavy metals promote cancer progression by inducing oxidative stress and DNA damage. This leads to uncontrolled cell growth and reduces the effectiveness of cancer therapies. Cadmium and arsenic are particularly dangerous, as they interfere with glucose metabolism and other critical biochemical processes, accelerating malignancy and increasing treatment resistance [15].

2.3 Biomonitoring: Hair Analysis for Heavy Metal Exposure

While blood and urine are commonly used for detecting toxic metals, hair analysis is gaining popularity due to its ability to provide long-term exposure data. Hair samples offer insights into metal accumulation over time, making them useful for monitoring environmental contamination, drug use, and prenatal toxin exposure.

Hair analysis is particularly effective for detecting exposure to arsenic, cadmium, lead, and chromium. This method aids in identifying contamination sources and implementing preventive measures to minimize exposure risks [16-17].

2.4 Metals in Growth, Development, and Metabolism

Zinc is essential for growth, immune function, vitamin A utilization, and hormone production (e.g., insulin). Manganese is critical for fetal and early childhood development, influencing skeletal formation and neurological health. Chromium plays a vital role in glucose, lipid, and protein metabolism, making it essential for maintaining metabolic balance. Deficiencies in these metals can lead to developmental abnormalities and chronic metabolic diseases [18].

3. Different Methods of Heavy Metal Detection

Rapid and precise detection of metal ions is crucial in today's environment, where heavy metal pollution poses significant risks. Traditional methods such as High-Performance Liquid Chromatography (HPLC), Inductively Coupled Plasma (ICP), Electrochemical techniques, and Optical methods are widely used. Additionally, advancements in sensor technology, including chemically and biologically based sensors, as well as the integration of nanoscience with electrochemical methods, have gained significant attention. This section reviews the principles, applications, advantages, and limitations of these detection methods [19].

3.1 High-Performance Liquid Chromatography (HPLC)

Since its development in the late 1960s and early 1970s, HPLC (high-performance liquid chromatography) has grown to be a fundamental aspect of analytical chemistry. It is extensively utilized for the separation, verification, and quantification of chemicals in sectors like food, biotechnology, medicines, and environmental monitoring. Based on how a mixture's constituent parts interact with both a stationary phase & a mobile phase, HPLC separates them. After the sample is inserted, a liquid known as the mobile phase passes through a column filled with stationary phase. Each component's retention duration varies according to how well it binds to the stationary phase. allowing for separation [20].

Advantages

- Versatility: able to examine a variety of substances, including thermally and non-volatile molecules.

- Superior Sensitivity: Capable of detecting trace amounts of analytes.
- Quantitative Analysis: Provides accurate quantification of target compounds using reference standards.

Applications

- Pharmaceuticals: Drug development and quality control.
- Environmental Monitoring: Detection of pollutants in water and soil.
- Food Safety: Analysis of nutrients and contaminants.

Limitations

- Complexity: Requires skilled operators and sophisticated equipment.
- Sample Preparation: Often involves extensive sample preparation.
- Cost: High initial investment and maintenance costs.

Recent Innovations

- Miniaturization: Development of micro- and nano-HPLC systems.
- AI Integration: Use of artificial intelligence for data analysis and method optimization [21].

3.2 Inductively Coupled Plasma (ICP) Techniques

3.2.1 Inductively Coupled Plasma Optical Emission Spectrometry (ICP-OES) Principle

ICP-OES uses a high-temperature plasma (up to 8,000 K) to atomize and excite sample elements. The excited atoms emit light at characteristic wavelengths, which is detected and quantified [22].

Advantages

- Multi-Element Analysis: Can detect multiple elements simultaneously.
- Wide Dynamic Range: Suitable for analysing a broad range of concentrations.
- High Sensitivity: Capable of detecting trace elements.

Limitations

- Interference: Matrix effects can affect signal intensity.
- Cost: Expensive instrumentation and operational costs.
- Sample Preparation: Requires preconcentration for low-concentration samples.

Applications

- Environmental Analysis: identifying of heavy metals in water and soil.
- Clinical Analysis: Trace element analysis in biological fluids [23-25].

3.2.2 Inductively Coupled Plasma Mass Spectrometry (ICP-MS)

ICP-MS uses mass spectrometry and plasma ionization to identify ions by calculating their mass-to-charge ratio.

. It offers extremely high sensitivity and can detect elements at ultratrace levels [26]

Advantages

- Ultra-Low Detection Limits: Capable of detecting elements at sub-pg/L levels.
- Isotopic Analysis: Can differentiate between isotopes of the same element.
- Multi-Element Capability: Simultaneous detection of multiple elements.

Limitations

- Isobaric Interferences: Overlapping signals from different elements.
- Cost: High initial and operational costs.
- Complexity: Requires skilled operators.

Applications

- Geological Analysis: Isotopic analysis of rocks and minerals.
- Clinical Research: Trace element analysis in biological samples [27- 33].

3.3 Electrochemical Methods

Electrochemical methods are cost-effective, portable, and suitable for on-site monitoring of heavy metals. These techniques measure changes in electrical signals (current, voltage, impedance) caused due to the existence of metal ions in a solution [34-35].

3.3.1 Potentiometric Techniques

- *Principle:* Determines the difference in potential between a reference electrode and a working electrode.
- *Advantages:* Low cost, rapid response, and good selectivity.
- *Limitations:* Lower sensitivity compared to other methods.
- *Applications:* Detection of heavy metals in water and soil [36].

3.3.2 Voltammetric Techniques

- *Principle:* Measures current as a function of applied voltage. Common techniques include three types of voltammetry: anodic stripping, differential pulse, and cyclic.
- *Advantages:* High sensitivity, low detection limits, and suitability for multi-element analysis.
- *Applications:* Detection of heavy metals in environmental and biological samples [37-42].

3.3.3 Amperometry

- *Principle:* Measures current at a fixed potential.
- *Advantages:* Simple and rapid.
- *Limitations:* Limited to single-element detection.
- *Applications:* Detection of electroactive species in solution [43-44].

3.3.4 Chronocoulometry

- *Principle:* Measures the total charge transferred during an electrochemical reaction.
- *Advantages:* High signal-to-noise ratio.
- *Applications:* Analysis of heavy metals in complex matrices [45-46].

3.4 Optical Methods

3.4.1 Atomic Absorption Spectrometry (AAS)

AAS calculates how much light is absorbed by atoms that are free in a state of gas. A flame is used to atomize the sample, and the amount of light absorbed at particular wavelengths is measured. [47-48].

Advantages

- High Selectivity: Specific to individual elements.
- Low Detection Limits: Suitable for trace analysis.
- Cost-Effective: Lower operational costs compared to ICP techniques.

Limitations

- Single-Element Analysis: Limited to one element at a time.
- Matrix Effects: Can interfere with accuracy.

Applications

- Environmental Monitoring: Detection of heavy metals in water and soil.
- Clinical Analysis: Trace element analysis in biological samples [49-52].

3.4.2 Atomic Emission Spectrometry (AES)

When excited atoms returned to their ground state, the light they emit is measured by AES. The element's concentration is directly correlated with the light's intensity.

Advantages

- Multi-Element Analysis: Can detect multiple elements simultaneously.
- High Sensitivity: Ideal for analysis of trace amount.

Limitations

- Interference: Matrix effects may have an impact on accuracy
- Cost: Expensive instrumentation.

Applications

- Environmental Analysis: Detection of heavy metals in water and soil.
- Industrial Analysis: Quality control in metal production [53].

3.4.3 Laser-Induced Breakdown Spectroscopy (LIBS)

LIBS produces plasma on the sample's surface using a highly energetic laser pulse. The elemental composition is ascertained by analyzing the light that is released. [54-55].

Advantages

- Rapid Analysis: Minimal sample preparation required.
- Portability: Suitable for field applications.
- Multi-Element Capability: able to identify several items at once.

Limitations

- Lower Sensitivity: In contrast with ICP and AAS techniques.
- Matrix Effects: Can affect accuracy.

Applications

- Environmental Monitoring: On-site detection of heavy metals.
- Industrial Analysis: Quality control in metal production [56-59].

3.4.4 X-Ray Fluorescence (XRF)

When a sample gets excited using a primary X-ray source, XRF detects the secondary X-rays that are released by the sample. Every element releases X-rays at distinct energies [60-61].

Advantages

- Non-Destructive: Does not require sample preparation.
- Multi-Element Analysis: Can detect multiple elements simultaneously.

Limitations

- Lower Sensitivity: Compared to ICP and AAS techniques.
- Matrix Effects: Can affect accuracy.

Applications

- Environmental Analysis: Identification of most heavy metals in water and soil
- Archaeology: Analysis of ancient. Artifacts [62-63]

3.4.5 UV-Vis Spectrophotometry

UV-Vis spectrophotometry evaluates what amount of visible or ultraviolet light a sample absorbs. The absorption has a direct relation to the analyte's concentration. [64].

Advantages

- Cost-Effective: Low operational costs.
- Simplicity: Easy to use and widely available.

Limitations

- Lower Sensitivity: Compared to AAS and ICP techniques.
- Interference: Matrix effects can affect accuracy.

Applications

- Environmental Monitoring: Detection of heavy metals in water.
- Food Safety: Analysis of contaminants in food [65-66].

3.5 Electrochemiluminescence (ECL)

ECL involves the generation of light from electrochemical reactions. Reactive intermediates are formed at the electrode surface, which then emit light upon relaxation [67-68].

Advantages

- High Sensitivity: Suitable for trace analysis.
- Selectivity: Can be tuned for specific analytes.

Applications

- Clinical Analysis: Detection of biomarkers.
- Environmental Monitoring: Detection of heavy metals [69-73].

4. Fluorescence Techniques

Fluorescence is the phenomenon that occurs when some compounds produce radiation when exposed to a light beam. This instantaneous process begins when light is absorbed and stops when the incident light is turned off. Fluorescent compounds are those that exhibit the fluorescence phenomena. Therefore, the capability of numerous substances to absorb one wavelength of light and then give an alternative wavelength of light instead of it is known as fluorescence. Compared to absorption approaches, fluorescence methods are more adaptable. Both emission and absorption wavelengths can be employed in fluorescence. Interference can also be avoided by selecting wavelengths other than the maximum. The quick increase or decrease of portions of a spectrum, however, can produce mistakes during spectrometric

absorption procedures, which lowers sensitivity. There are no such limitations with the fluorescence approach. Compared to absorbance procedures, fluorescence methods are around 100 times more expensive. If their respective excitation wavelengths are far enough apart, two components that emit the same fluorescence color can be identified simultaneously using fluorescence methods.

Applications

- Uranium in Salts Determination: Nitric acid is used to oxidize the uranium-containing sample. Sodium fluoride and the oxidized sample are combined to produce a melt that is subsequently cooled to a glassy, solid state. A fluorimeter that has been particularly designed is used to examine this. This technique can identify uranium at concentrations between 5×10^{-9} g per gram of solid material.
- Investigation of Inorganic Ions: These ions typically don't glow. Nonetheless, it has been discovered that certain inorganic ions combine with non-fluorescent organic molecules to generate fluorescent chelates. This process allows for the analysis of most of the transition elements.
- Fluorescent Indicators: The pH affects the color and intensity of fluorescent indicators. Acid-base titrations make use of these indicators. These can be applied to colored solutions whose color change is difficult to observe during titration.
- Organic Analysis: Determining vitamin B1 (thiamine), vitamin B2 (riboflavin), and quinine are a few crucial uses in organic analysis.
- Tryptophan, uric acid, warfarin, indole, skatole, guanidine, cysteine, anthranilic acid, aromatic polycyclic hydrocarbons compounds and other substances can also be determined with its help. Fluorometric techniques can be used to determine even pharmaceutical drugs (Adrenaline, pencillin, phenobarbital, chloroquin, etc.) and plant-based products (e.g., folic acid, ascorbic acid, chlorophyll, ergot, etc.) [74].

Advantages

- Quick, sensitive, and highly accurate detection of heavy metal ions
- They are simple to include into microfluidic systems.
- utilized to keep an eye on hazardous situations
- rapid reaction times, with minimal detection limits, simple and easy technology

Since the change in fluorescence brought on by coordination occurs rapidly and is non-destructive, specific, highly sensitive, and screenable, techniques based on fluorescence detection using tiny molecules are appropriate.

These techniques focus on creating and developing fluorophores with the binding mechanism and coordination ligands required to identify metal ions in solution. The key fluorophores—rhodamine, the pyrene, anthracene, naphthalimide, aminoquioline, bithiophene, & coumarin—are coupled with the appropriate probes to provide fluorescent sensors for Hg^{2+}, Cu^{2+}, Zn^{2+}, Cd^{2+}, Fe^{3+}, $Ni^{2+,}$ as well as Cr^{2+} [75].

5. New Developments in Colorimetric and Fluorescent Sensors for Metals Ion Detection

Bibo Zhang et al. successfully prepared Quinaldic acid chloride and 2-aminobenzimidazole stirred in anhydrous dichloromethane (CH_2Cl_2) to create **QLBM** sensor **(Fig. 1)**.

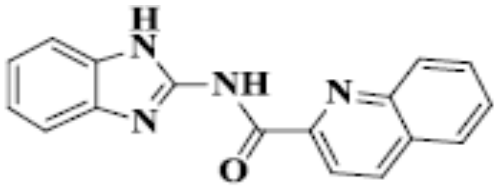

Fig. 1: Chemical structure of QLBM sensor

For metal ion concentrations in the range of 0–50 μM, there was a strong linear association with fluorescence intensity. For Cu^{2+} and Fe^{3+}, the corresponding limit of detection were 1.35×10^{-7} M & 1.24×10^{-7} M, respectively. QLBM exhibited low cytotoxicity (cell viability >90% at 20 μM), making it suitable for living cell imaging applications to detect Cu^{2+} and Fe^{3+} ions in biological systems [76].

Aniket Chaudhari et al. introduced two brand-new pyrene-based turn-off sensors, called APSS (sodium (E)-4-hydroxy-3-((pyren-1-ylimino) methyl) benzenesulfonate) and APTS (sodium 8-aminopyrene-1,3,6-trisulfonate) (Fig. 2), They enable their application in pure water samples by including sulfonate groups.

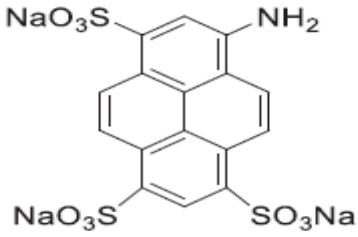

(APTS)

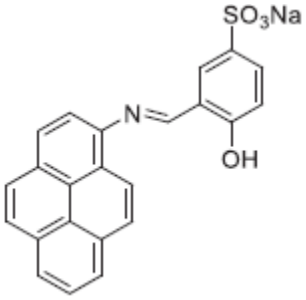

(APSS)

Fig. 2. Chemical structure of APTS and APSS Sensors

The Stern-Volmer plot shows that the APTS sensor exhibits a linear quenching behavior with an extremely high quenching constant of 46.09 μ M. This indicates the sensor's affinity for Fe^{3+} ions is high. With a LOQ of 153 nM and a LOD of 45.9 nM (R2 = 0.982), comparable quantitation results were found for APSS. The sensor's fluorescence response became more specific due to the binding pocket of the imine group. To look into the quenching mechanism, fluorescent lifetime spectra were captured for both sensors with and without the Fe^{+3} ion. The fluorescence lifetime (τ) diminished because a quencher was present for both sensors, as revealed by their spectra. When Fe^{3+} ions were present, the fluorescence lifetime of APTS was lowered to 2.21 ns from 6.06 ns. The two sensors were used to find Fe^{+3} ions in real samples of the environment, such tap and lake water [77].

Süreyya Oğûz Tümay et al. synthesized an acetohydrazide derivative based on naphthalene, which was employed as a fluorescent probe for aluminum ion detection in real samples. The modest fluorescence emission observed in this compound was attributed to the photoinduced electron transfer (PET) and excited-state intramolecular proton transfer (ESIPT) mechanisms involving the imine (–C=N–) bond, phenolic –OH, and naphthalene moiety. The fluorescence emission characteristic was based on a Schiff base system. For Al^{3+} detection (Scheme 1), the sensor exhibited a linear effective range of 1.00–20.00 mmol L^{-1} and a limit of detection equal 0.34 mmol/ L. The sensor's performance was evaluated through spike and recovery analysis in drinking water, seawater, and urine samples [78].

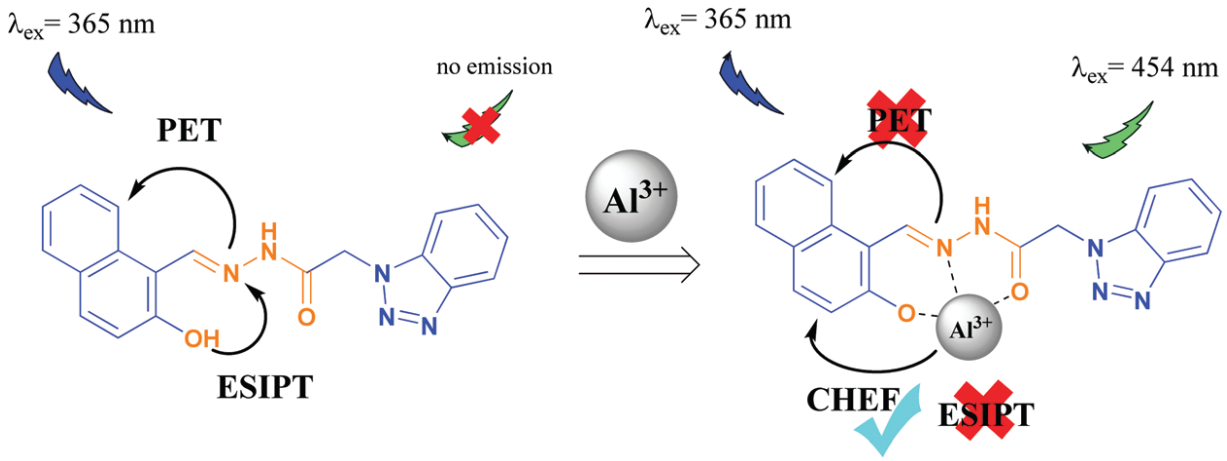

Scheme 1: The proposed interaction and fluorescence sensing mechanism for proposed compound with Al^{3+} ions.

Yunfei Liang et al. presented a novel photochromic diarylethene derivative incorporating an ethylimidazo[2,1-b]thiazole-6-hydrazide unit, with limit of detection equal 2.97 × 10^{-9} mol/ L for both Zn^{2+} & Al^{3+}. The results of ^{1}H-NMR titration studies show that C=N isomerism happens when sensor 1O becomes complexed with aluminum ion; only the proton signals of –OH at 11.82 ppm totally vanish when Zn^{2+} is added to 1O. An excited state intramolecular proton transfer (ESIPT) mechanism, enhanced chelation fluorescence (CHEF), and C=N isomerization can all be responsible for fluorescence amplification. Because of the ESIPT and C=N isomerization (nonradiative quenching), 1O displays a very low fluorescence intensity when it is provided in an unbound form. The complex 1O–Al^{3+} was created when aluminum ion was added to 1O. This complex stops 1O from isomerizing in the C=N direction. Thus, stable Al^{3+} complexation with 1O may cause rigidity in the final complex, leading to effective chelation increased fluorescence. Nonetheless, the intramolecular charge transfer (ICT) pathway, which was hindered from the ethylimidazo [2,1-b] thiazole-6-hydrazide group to the diarylethene unit, may be responsible for the increase in fluorescence brought on by 1O in reaction to Zn^{2+}. This sensor was used for estimating the quantities of aluminum ions and zinc ions in actual samples of water [79].

Yuan Zhang et al. developed a sensor, (Z)-N-((pyren-4-yl)methylene)(furan-2-yl)-methanamine (BF) (Fig. 3), for Al^{3+} detection by a mechanism based on a monomer /excimer switch mechanism. The proposed interaction between BF and Al^{3+} was investigated using ^{1}H NMR spectroscopy, with a limit of detection reach 1.04 mmol L^{-1} in the range of 1–35 mmol/L. The involvement of oxygen atoms from the furan and imine groups in Schiff base complexation with Al^{3+} likely induced a folded conformation, aligning the pyrene moieties in a face-to-face orientation High pyrene excimer emission replaced poor pyrene monomer emission as a result of this conformational change. Additionally, paper strip testing demonstrated the potential practical applications of the BF chemosensor [80].

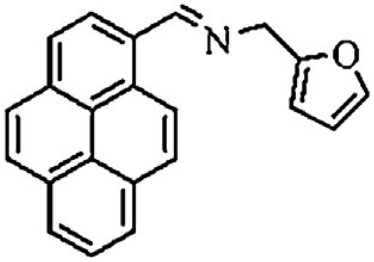

Fig. 3: Chemical structure of (Z)-N-((pyren-4-yl)methylene)(furan-2-yl)-methanami-ne (**BF**)

Yang Wang et al. developed a novel turn-on chemosensor with two functions, 2,6-diformyl-4-methylphenol-di(isoquinolinyl-1-hydrazone) (HL) (Fig. 4), capable of highly selective detection of magnesium ions and zinc ions in various solvent systems. The sensor exhibited exceptionally low limits of detection of 3.07×10^{-7} M for magnesium ion and 2.97×10^{-8} M for zinc ions, highlighting its potential for sensitive ion recognition.

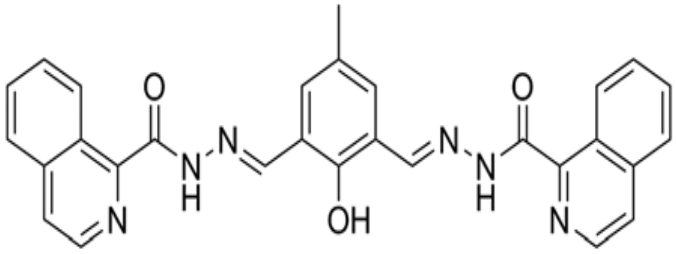

Fig. 4: Chemical structure of 2,6-diformyl-4-methylphenol-di(isoquinolinyl-1-hydrazone) (HL)

HL was utilized as a fluorescent probe to detect zinc levels in zinc sulfate syrup, demonstrating its effectiveness in real sample analysis. Additionally, it was applied for measuring Mg^{2+} concentrations in natural drinking water sources, including Luyuanquan drinking water, further validating its practical applicability [81].

Qing-Ming Wang, et al. created a fluorescent and colorimetric sensor (NT) (Fig. 5) based on a naphthaldehyde derivative for Al^{3+} detection, exhibiting a linear range of 0 - 10 µM and a limit of detection 1.1×10^{-7} M [82].

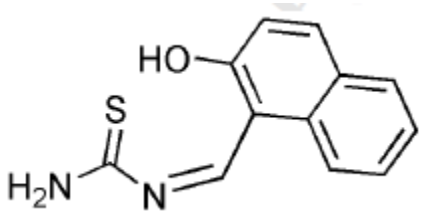

Fig. 5: Chemical structure of naphthaldehyde 1-((2-hydroxynaphthalen-1-yl)methylene)thiourea (NT)

Wenjie Feng et al. synthesized probe L through a one-step amide reaction between free N-terminal dopamine and (anthracen-9-ylmethylsulfanyl) acetic acid, achieving a limit of detection 1.1×10^{-6} M for Hg^{2+}.

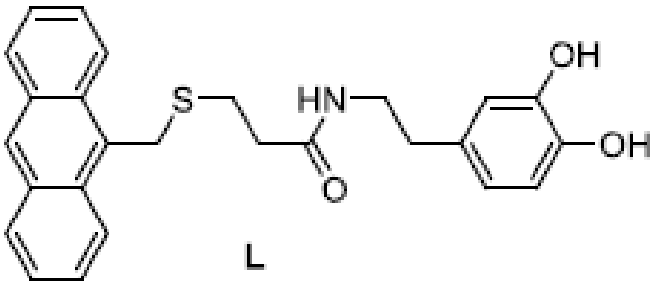

Fig. 6. Chemical structure of L sensor

The ^{1}H-NMR spectra of probe L (Fig. 6), analyzed with and without Hg^{2+}, revealed the disappearance of phenol proton peaks and shifts in methylene proton peaks, indicating coordination between Hg^{2+} and both the sulfur and catechol groups of L. Further confirmation was achieved by oxidizing the catechol group to quinone with H_2O_2, as evidenced by a decrease in the absorption band in the HEPES buffer solution of L.

In the quinone form of L, Hg^{2+} shows a negligible change in fluorescence, suggesting that the sulfur atom and catechol group both engage in coordination, with the catechol group mostly responsible for the chelation-enhanced fluorescence shift. This makes L a promising probe for monitoring low levels of Hg^{2+} in samples from the environment and biological imaging [83].

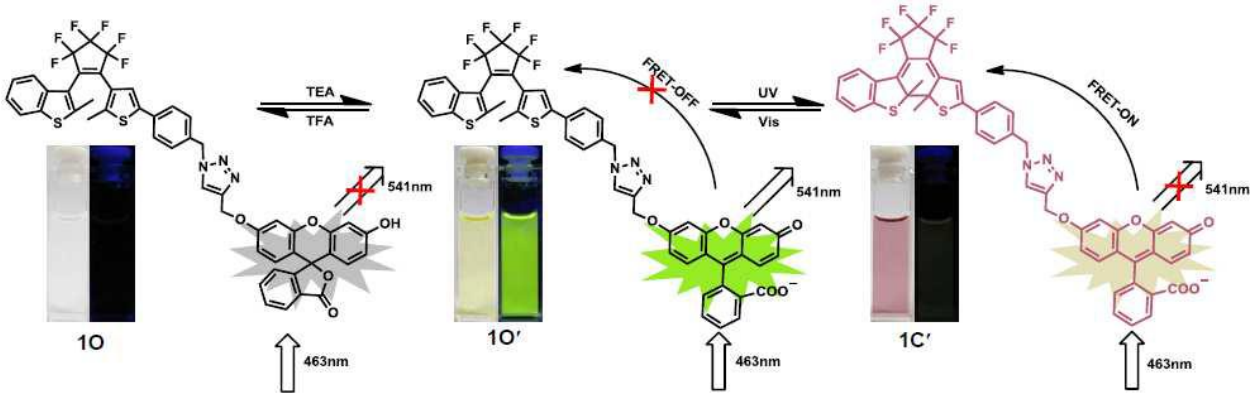

Scheme 2: The proposed interaction and fluorescence sensing mechanism for proposed compound with Cu^{2+} ions.

Lele Ma et al. produced by synthesizing a novel photochromic molecule (1O) by integrating fluorescein with a diarylethene core via a triazole linkage. The resulting molecule exhibits dual-controllable fluorescence properties modulated by the stimuli of acid/base and light, enabling its use as a molecular switch in a three-input, three-output digital circuit. Additionally, in the presence of $AscH^-$, 1O functions as a Cu^{2+} detection using a "turn-on" fluorescent chemosensor (Scheme 2), demonstrating the potential of photochromic diarylethene structures in designing advanced fluorescent chemosensors [84].

B. Kirthika Rani et al. synthesized the sensor PYMH {N1',N3'-bis(pyren-1-yl)ethylene) malonohydrazide} (Fig. 7) in two easy processes, which include making

malonohydrazide and symmetrical pyrene malonohydrazide with pyrene units on both sides. The sensor demonstrated a very small limit of detection (LOD) of 5.1 nM, highlighting its potential for sensitive analytical applications.

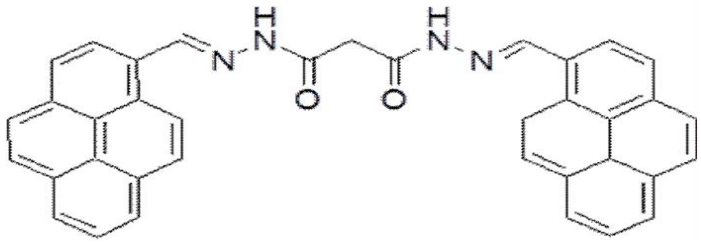

Fig. 7. Chemical structure of PYMH sensor

The ^{1}H-NMR analysis of PYMH before and after Zn^{2+} addition revealed downfield shifts in the methylene, pyrene, and imine proton signals, indicating complexation. The persistence of NH proton signals confirmed that NH was not involved in binding, while imine nitrogen and carbonyl oxygen played key roles in coordination. Fluorescence microscopy studies further demonstrated the sensor's potential for Zn^{2+} detection in living cells [85].

Ping Zhang et al. introduced the synthesis of H_4L (Fig. 8), a sensor molecule with a minimum limit of detection 4.87×10^{-7} M, exhibiting strong luminescence due to its coumarin groups and a push-pull electron system. The molecule contains −OH, which is an excellent electron donor, and a C=N bond, acting as an electron-withdrawing group. When Cr^{3+} and Al^{3+} ions are introduced into its N_2O_2 binding sites, intramolecular charge transfer (ICT) occurs, leading to fluorescence quenching because of the C=N bond's isomerization. When S^{2-} is added to the L−Cr^{3+} framework, the stronger binding affinity of S^{2-} to Cr^{3+} causes the displacement of Cr^{3+} from H_4L, restoring fluorescence and enabling selective S^{2-} detection. The probe demonstrated minimal variation across physiological pH values, indicating its potential application in biological and environmental monitoring. The L−Cr^{3+} system was effectively used to identify S^{2-} in tap.

river, and distilled water samples, proving its efficiency in real-world applications [86].

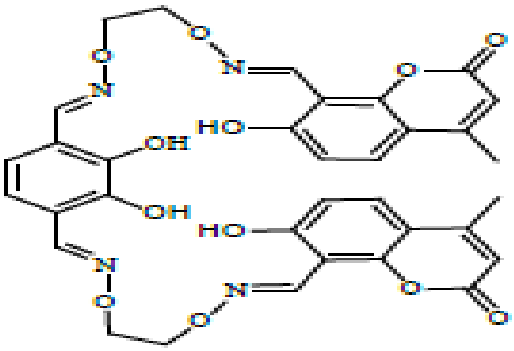

Fig. 8. Chemical structure of H_4L sensor

Ping Li et al. synthesized a novel fluorescent sensor, N' -[(2-hydroxyphenyl)methylidene]imidazo[1,2-a]pyridine-2-carbohydrazide (S), through condensation by Schiff-base between imidazo[1,2-a]pyridine-2-carbohydrazide and salicylaldehyde, achieving a very small limit of detection reach to 4.55×10^{-11} M. The photoinduced electron transfer (PET) phenomenon was suppressed upon the addition of Al^{3+} (Scheme 3), leading to significant fluorescence recovery through the highly efficient chelation-enhanced fluorescence (CHEF) effect, indicating strong binding between Al^{3+} and S [87].

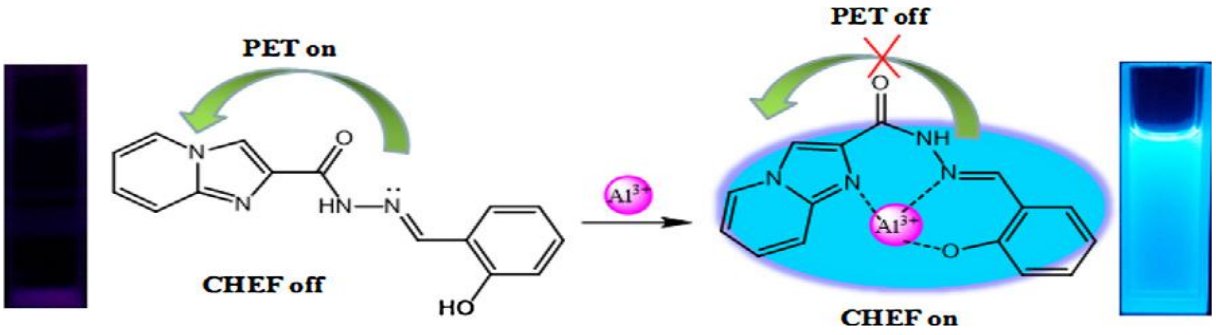

Scheme 3: The proposed interaction and fluorescence sensing mechanism for proposed compound with Al^{3+} ions.

Hao Fang et al. described probe L (Fig. 9), An extremely sensitive one fluorescent probe for Zn^{2+} and Cu^{2+} detection, based on p-dimethylaminobenzoyl derivatives, with a detection limit of (LOD) of 45 nM for Zn^{2+} and 17 nM for Cu^{2+}. Probe L was applied to determine Cu^{2+} and Zn^{2+} concentrations in drinking water, tap water, and human blood, utilizing test paper technology for real sample analysis. These findings suggest that probe L holds potential for chemical and environmental applications in detecting Cu^{2+} and Zn^{2+} [88].

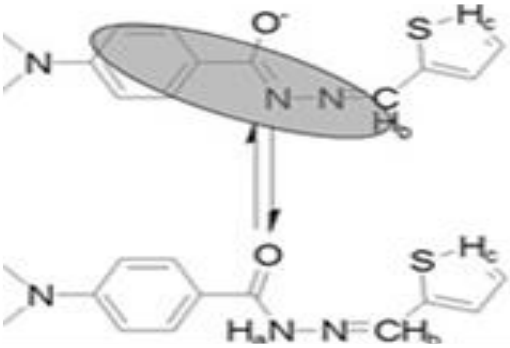

Fig. 9. The structure and synthesis process of the probe L.

Yinglong Fu et al. described 1-(3,5-Dimethyl-4-isoxazolyl)-2-{2-methyl-5-[4-hydroxyl-3-salicylhydrazone-phenyl]-3-thienyl}perfluorocyclopentene (1O) (Fig. 10), a newly synthesized photochromic diarylethene-based sensor incorporating a salicylhydrazide Schiff base unit. The sensor demonstrated fluorescence and photochromic properties, with detection limit of (LOD) values of 8.31×10^{-8} mol/L for Aluminum ions and 3.33×10^{-7} mol /L for Zinc ions. The detection mechanism involved Chelation-enhanced fluorescence (CHEF), C=N isomerization, and excited-state intramolecular proton transfer (ESIPT). By chelating 1O with Al^{3+}, ESIPT and C=N isomerization was preventable, stabilizing the molecular structure and leading to enhanced fluorescence intensity. Additionally, 1O exhibited a fluorescence switch upon photoirradiation. The 1O sensor might be a useful chemosensor for imaging Aluminum & zinc in cells of living organisms when applied to human cervical HeLa carcinoma cells [89].

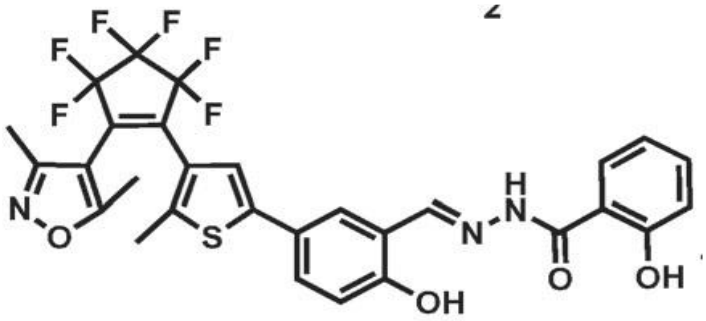

Fig. 10: The chemical structure of 1-(3,5-Dimethyl-4-isoxazolyl)-2-{2-methyl-5-[4-hydroxyl-3-salicylhydrazone-phenyl]-3-thienyl}perfluorocyclopentene (1O) sensor

Hanyu Wang et al. synthesized (N'-[(Z)-1H-indazol-3-ylmethylidene][2,1-b][1,3]benzothiazole-2-carbohydrazide (WS1) (Fig. 11) as a basic fluorescent chemosensor. The linear detection range of the sensor was demonstrated from 0 - 5×10^{-5} M with a limit of detection (LOD) of 4.32×10^{-8} M. In real water samples, WS1 demonstrated high efficiency for the quantitative determination of cupper ions [90].

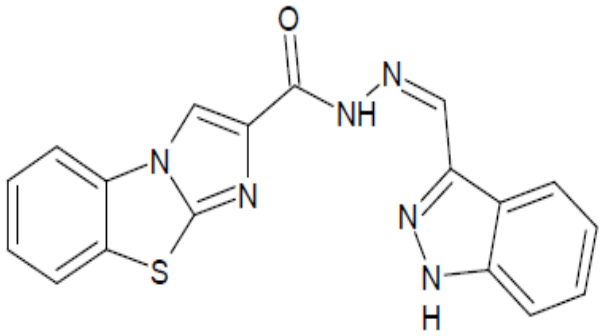

Fig. 11: The chemical structure of WS1 sensor

Lakshman Patra et al. presented 3-(((2-hydroxy-4-methylphenyl)imino)methyl)-[1,10-biphenyl] 4-ol (H_2L) (Fig. 12) as a fluorogenic chemosensor for the efficient determination of Zinc, Aluminum, and Fluorine ions, with detection limits of (LOD) of 2.24×10^{-7} M, 4.1×10^{-8} M, and 3.7×10^{-8} M, respectively. The weak fluorescence intensity of H_2L in its free state is attributed to intramolecular proton transfer (ESIPT) and C=N isomerization, which are suppressed upon coordination with metal ions, leading to a significant fluorescence enhancement via the chelation-enhanced fluorescence (CHEF) effect. A paper strip test was employed for the on-site visual detection of aluminum and zinc, where fluorescence color changes were observed upon exposure to UV light, although the detection limit (0.1 mM) was lower compared to the solution phase [91].

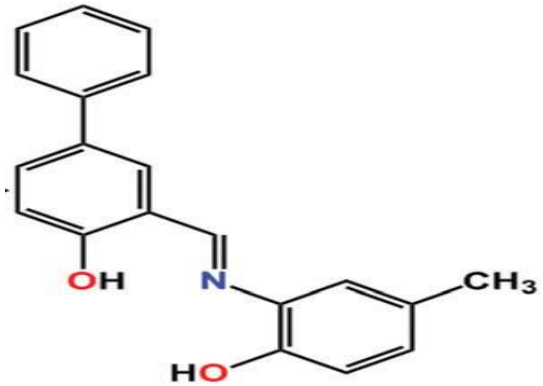

Fig. 12: The chemical structure of H_2L sensor

Mohammad Dodangeh, et al, used a 4-amino-1,8-naphthalimide-conjugated polyamidoamine dendrimer for detection of Ag^{+} ion with detection range of 0.3×10^{-4} - 4.8×10^{-4} M. The structure of PAMAM dendrimer modified with 4-amino-1,8-naphthalic anhydride. The dendrimer molecule

(Fig. 13) and the naphthalimide units are covalently bound, as can be observed. As a receptor site, the amido groups found at the internal region of the PAMAM dendrimer can interact with the Ag^{+} cations. When the naphthalimide moieties are conjugated with the PAMAM dendrimer, a It is possible to create a colorful, fluorescent molecule with significant fluorescence properties and photo-induced electron transfer.

. The photophysical properties of the created dendrimer were assessed considering its potential use as a PET sensor for the identification of different cations (Scheme. 4) [92].

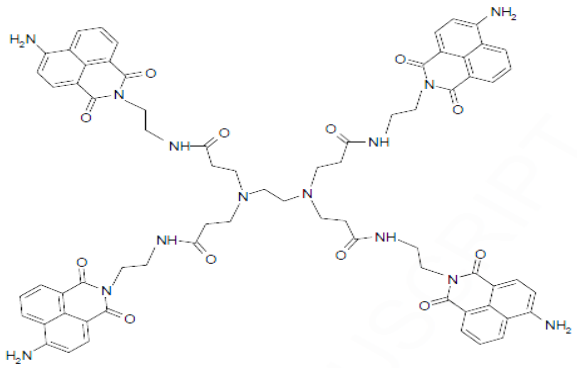

Fig. 13. The chemical structure of synthesized dendrimer.

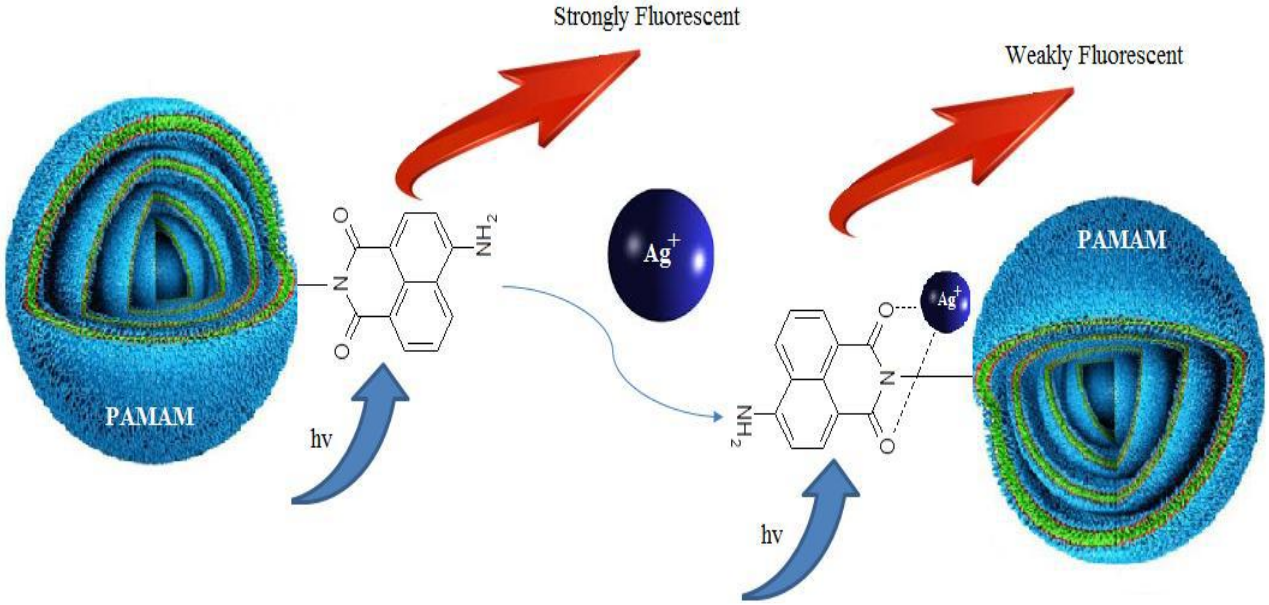

Scheme. 4 Schematic presentation of coordination of monomeric 4-amino-1,8-naphthalimide-conjugated PAMAM dendrimer with metal cations.

Gang Zhao, et al. designed and manufactured effectively a novel multifunctional chemo-sensor (RHCS-NH2) through the integration of Schiff base, rhodamine B hydrazide, and hydrazine hydrate group into triazine. The RHCS-NH_2 (Fig. 14) sensor was discovered to exhibit instantaneous multi-response to both Ca^{2+} and Zn^{2+} ions. The linear range for identifying calcium ions is 0.01- 10.0 µM, while for Zn^{2+} ions is 0.03~10.0 µM. The detection limits for Ca^{2+} and Zn^{2+} were calculated to be 0.10 nM & 0.14 nM, correspondingly.

The FTIR spectrum was acquired to confirm the hypothesized process even further. The peak associated with The FTIR spectra of RHCS-NH2's exhibited that, the absorption peak assigned to carbonyl moved to a lower frequency when chelating with zinc ions or calcium ions. When Zn^{2+} or Ca^{2+} ions were introduced to the solution, the peaks that are attributed to absorption of the hydroxyl group of RHCS-NH_2 (Ar-OH) moved to a lower frequency and had a band with a weak strength. Additionally, the bending vibration peak (Ar-OH) exhibits a blue shift and a peak with greater intensity, indicating that the coordination of Zn^{2+}/Ca^{2+} ions includes the amide carbonyl oxygen belong to RHCS-NH_2. Those results indicated that there has been greater durability of reactions between metal ions and the amide carbonyl& hydroxyl groups of the Schiff-based molecules.

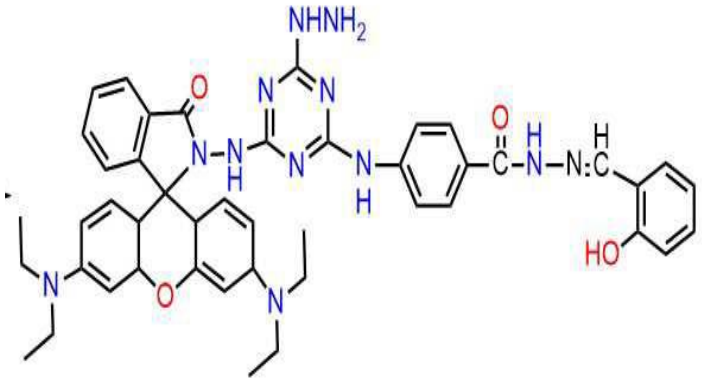

Fig. 14. The chemical structure of RHCS-NH_2 sensor

When metal ions (Zn^{2+} or Ca^{2+}) were added, it was discovered that the proton belonged to the hydroxyl (-OH) group departed. This phenomenon may be related to deprotonation and the creation of the metal coordination zinc ion complex. Specifically, the complicated mechanism in which the deprotonated oxygen group participates substantially induces a red-shift in the fluorescence spectra and an ICT process from the donor Schiff group to the acceptor Schiff-rhodamine moieties. A through-bond effect may be the cause of the upfield shift. Consequently, a binding model was put forth for the sensor complexation mechanisms of RHCS-$NH^{2+}Ca^{2+}$ and RHCS-$NH^{2+}Zn^{2+}$. Specifically, stable 5-membered condensed ring formation between the metal ion and oxygen or nitrogen of the Schiff base receptor in sensor molecules is responsible for the sensor's ability to recognize Ca^{2+} or Zn^{2+}. RHCS-NH_2 probe was applied to dual-channel concurrently detect calcium and zinc in three types of environmental water samples, including lake, mineral, and tap water [93].

Jinli Zhu et al. reported that the Schiff base CTS, created from 2-hydroxy-1-naphthaldehyde and 2-benzylthio-ethanamine (Fig. 15), functions as an effective turn-on fluorescence sensor for Zn^{2+} determination. This is attributed to the restricted rotation of the C=N bond relative to the naphthalene ring and/or the inhibition of the nitrogen atom's photo-induced electron transfer (PET) mechanism. CTS exhibited excellent selectivity for Zn^{2+} with a limit of detection 5.03×10^{-7} M. Furthermore, its potential for biological applications was demonstrated through Zn^{2+} detection in living cells [94].

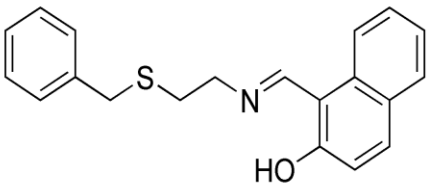

Fig. 15. The chemical structure of CTS sensor

Wei-Hua Ding, et al. developed and produced 1-[(1H-tetrazol-5-ylimino)methyl]naphthalen-2-ol (H_2L) (Fig. 16), a tetrazole derivative, as a fluorescent chemosensor for Zn^{2+} and Al^{3+}, the H_2L limit for detection aluminum ions was 5.86×10^{-6} mol /L , while, it was 1.81×10^{-6} mol L^{-1} for Zn^{2+}. After H_2L complexed with Al^{3+} ions, the ^1H NMR spectrum of H_2L was analyzed. The disappearance of the signal of the proton of naphthol hydroxyl indicated the binding mode of H_2L with aluminum ions. Likewise, the naphthol hydroxyl vanished and the CH=N proton signal moved downfield upon complexation with Zn^{2+} ions. For both systems, there was a minor shift in the other aromatic protons. The findings imply that the hydroxyl oxygen atom of H_2L and the imine nitrogen atom of Al^{3+} and Zn^{2+} are coordinated. Furthermore, the proton peaks did not significantly alter when Al^{3+} or Zn^{2+} were added to H_2L. H_2L's high sensitivity and selectivity for Zn^{2+} and Al^{3+} enabled its potential use in living cell bioimaging, as demonstrated in HeLa cancer cells [95].

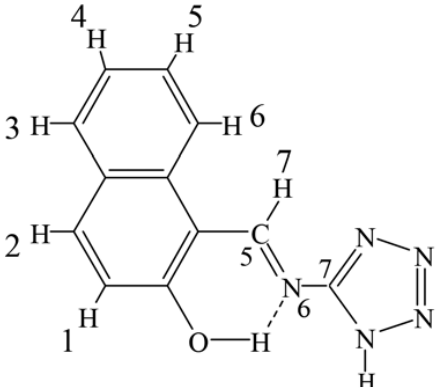

Fig. 16. The chemical structure of H_2L sensor

Guan-qun Wang et al. developed a novel sensor, isatin-3-(7'-methoxychromone-3'-methylidene) hydrazone (Fig. 17), using the chromone Schiff base to detect Mg^{2+}, with an estimated detection limit of approximately 5.16×10^{-7} M.

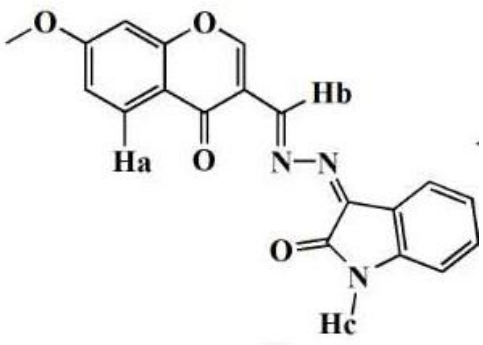

Fig. 17. The chemical structure of HL sensor

The chelation-enhanced fluorescence (CHEF) effect and the decrease in the PET effect are responsible for the probe's quick and observably increased reaction to the addition of Mg^{2+}. More precisely, a lone pair of electrons from the Schiff base caused the carbonyl group to quench the free receptor through photo-induced electron transfer (PET), resulting in the very faint fluorescent band that was seen. The chelation of the N and O atoms with Mg^{2+} upon the addition of Mg^{2+} led to an effective suppression of the PET process of the –CH=N– group [96].

Sellamuthu Anbu et al. synthesized a novel benzoyl hydrazone-based chemosensor (R) (Fig. 18) through Schiff base condensation of 2,6-diformyl-4-methylphenol with phenyl carbohydrazide. in aqueous applications it functions as an extremely specific fluorescence sensor for Cu2+ ions and Zn^{2+} ions.

The chemosensor R's fluorescence spectrum shows a moderate emission. The fluorescence emission is nearly entirely extinguished when higher amounts of aqueous Cu^{2+} solutions are gradually added to the solution of R. The dramatic quenching of the initial fluorescence intensity of R induced by the copper ion is caused by the reverse photoinduced electron transfer (PET) from the 4-methylphenyl moiety to the phenolic OH and

carbohydrazide nitrogen and oxygen atoms. This occurs because of the drop in electron density that occurs after Cu^{2+} ion complexation. On the other hand, the emission band was greatly boosted by the addition of Zn^{2+}, causing it to shift to a somewhat longer wavelength due to the Zn^{2+} ion. The completely filled d^{10} electronic configuration of the zinc ion, which typically does not include any electron-transfer or energy-transfer processes for deactivation of the excited state, could be the cause of the fluorescence amplification of R in the presence of zinc ion

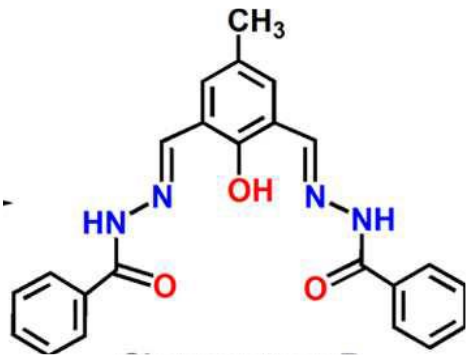

Fig. 18. The chemical structure of R sensor

Chemosensor R enables imaging of living cells of Cu^{2+} and Zn^{2+} ions, with limits of detection 17.3 and 16.5 ppb, respectively. Its membrane permeability and non-toxic nature make it a valuable probe for detecting these Ions in samples from the environment and biology [97].

Rabiul Alam et al. reported that the novel 3-hydroxymethyl-5- methylsalicylaldehyde-naphthyl hydrazone (H_3SAL-NH) exhibits ESIPT behavior because the azomethine Nitrogen atom in the state of excitation receives a proton transport via the phenolic OH group. The cis-trans isomerization come from the azomethine group and its ESIPT behavior cause the free ligand to become extremely faintly luminous. Nevertheless, coordination to the metal ions in the presence of zinc ions and aluminum ions blocks ESIPT and isomerization, turning on fluorescence for both ions. It was discovered that the LODs for zinc ions and aluminum ions were, respectively, 3.1 nM and 0.92 nM.

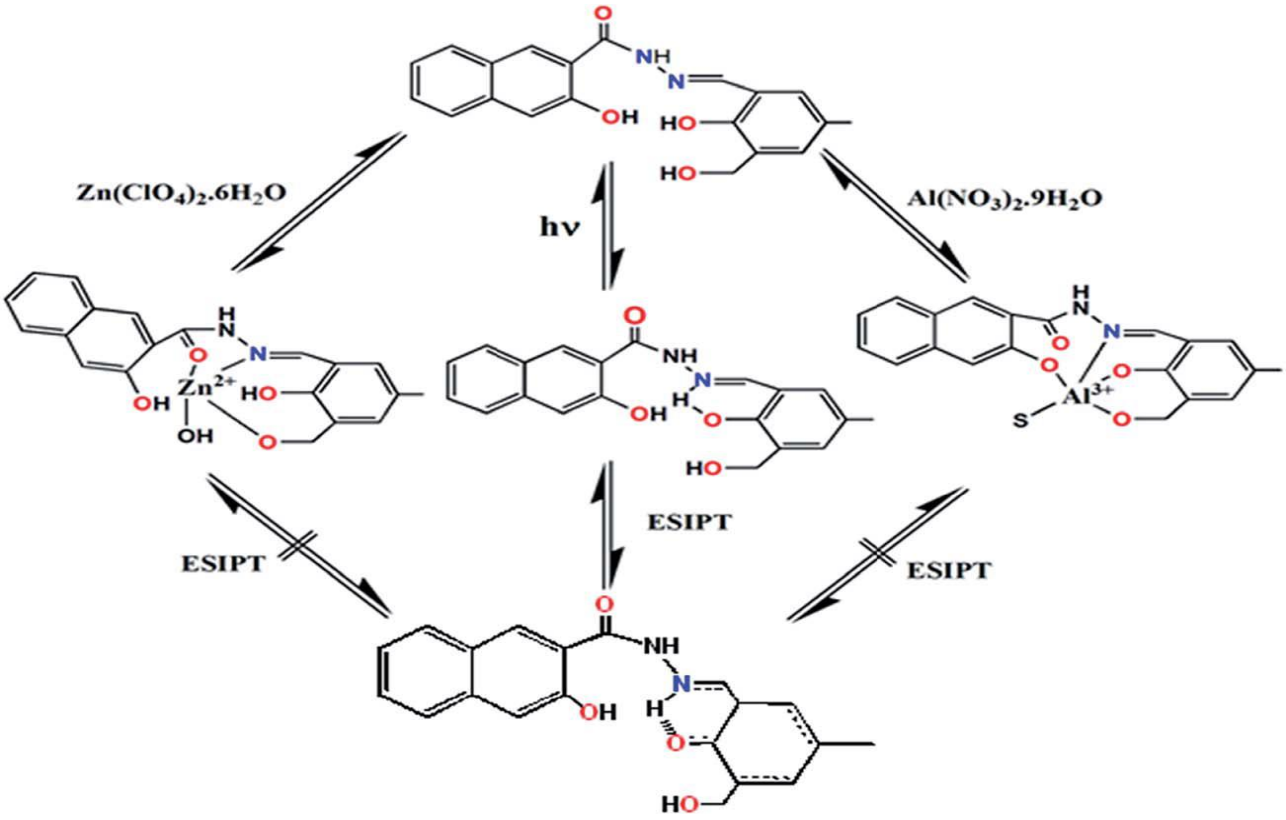

Scheme. 5 Schematic presentation of coordination of H_3SAL-NH with Zn^{2+} and Al^{3+} cations.

^{1}H-NMR investigations, which amply demonstrated a shift in proton of the azomethine coming from the free ligand's chemical changes in the presence of aluminum and zinc, correspondingly, provided additional evidence for the coordination modes. The OH proton on the free ligand's hydroxymethyl group disappears due to its significant participation in bonding with zinc ions, but the -NH proton and the other two OH protons remain unaltered due to their non-participating behavior. On the other hand, when aluminum ions is added, all three Hydroxyl protons disappear.

This makes it very evident that the OH protons are bonding with Al^{3+}, but the -NH proton is not shifting, indicating that it is not connecting with any metal ions. Therefore, we might therefore say that the hydroxymethyl group of H_3SAL-NH, one imine nitrogen atom, and two phenolate oxygen atoms are Participant

In the binding with Al^{3+}. However, in the case of the Zn^{2+} hydroxymethyl group, the hydroxo and amido oxygen atoms, one imine nitrogen atom, and the two phenolate oxygen atoms are not Participant in the binding (Scheme. 5). Cell imaging in vitro shown that it simply diffuses into cells and detects Zn^{2+} and Al^{3+} by forming stable complexes in trace amounts [98].

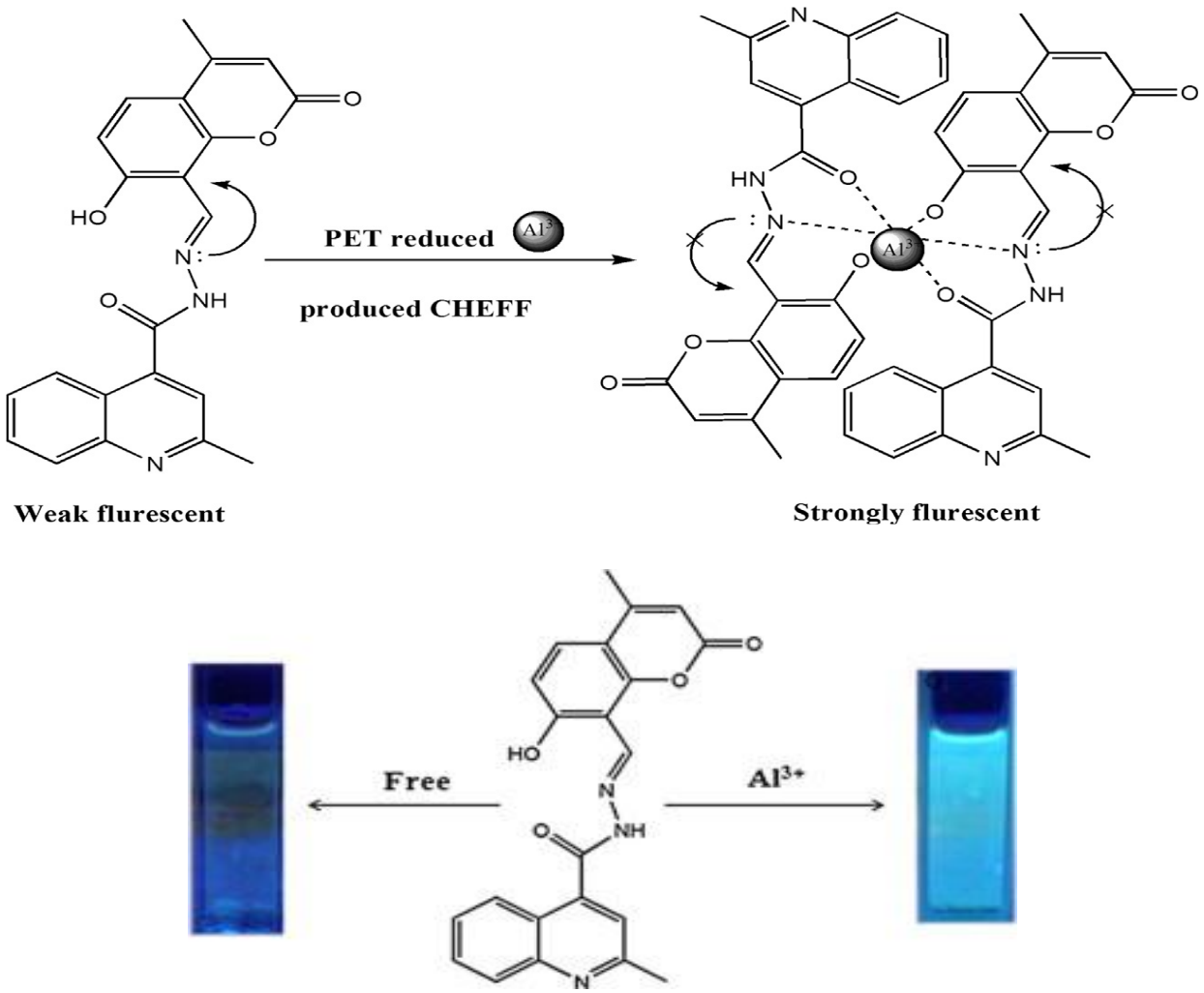

Scheme. 6 Schematic presentation of coordination of **L** with Al^{3+} ions.

Xinjian Cheng et al. designed and synthesized three tiny-molecule boron dipyrromethene (BODIPY) derivatives (B3a, B3b, and B3c) to develop macromolecular fluorescence sensors, incorporating them into polyurethane. These BODIPY Compounds showed remarkable specificity and sensitivity as well.

These compounds' color quickly changed when mercury ions, chromium ions, and iron ions were added. Their peaks of fluorescence also changed and became more intense. When B3a, B3b, and B3c were exposed to polyurethane (PU), their sensing qualities persisted. The macromolecular chains were modified by adding B3a, B3b, and B3c to create functional PU films. The color and fluorescence characteristics of B3a, B3b, and B3c are retained by the functional PU films. mercury ions, chromium ions, and iron ions could be found and separated using fluorescent PU films. Furthermore, these kinds of materials could both detect and eliminate ions of heavy

metal. It will have practical uses in environmental cleanup [99].

Jing-can Qin et al. developed a fluorescent sensor, 8-formyl-7-hydroxy-4-methylcoumarin-(2-methylquinoline-4-formyl) hydrazone (**L**). The least limit of detection for aluminum ions was determined to be 8.2×10^{-7} M.

Schiff base structures offer a hard-base environment for the hard-acid aluminum ions due to the nitrogen-oxygen-rich coordination atmosphere. A novel 'turn-on' fluorescent probe for detecting aluminum in ethanol, depended on coumarins, was investigated and explained by the chelation-enhanced fluorescence (CHEF) process. Oxygen chelation, which involves the nitrogen atom of the -C=N group, the oxygen atom of -C=O, and the oxygen of Ar-O with Al^{3+}, is responsible for the enhanced emission intensity of L in the presence of aluminum ions. This effectively inhibits the PET process of the -C=N group. Due to its low detection limit, this chemosensor holds potential for detecting micromolar levels of Al^{3+} within environmental and biological systems (Scheme. 6) [100].

Pornthip Piyanuch et al. developed a novel fluorescent probe (FC4) (Fig. 19) based on the fluorescein dithia-cyclic skeleton for detecting Hg^{2+} in an aqueous buffer solution. FC4 was synthesized using Kornblum oxidation, ester hydrolysis, alkylation, imine formation, and imine reduction. The sensor's limit of detection for Hg^{2+} was determined to be 7.38×10^{-9} M.

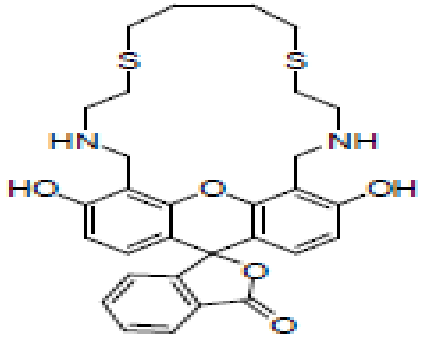

Fig. 19 Chemical Structure of sensor FC4

A semi-rigid framework preorganized the binding site of FC4, which contained sulfur and nitrogen atoms as donor atoms for a powerful and beneficial electrostatic bond with mercury ions, based on a methodology akin to host-guest supramolecular chemistry. Therefore, we anticipate that ion-dipole interactions between the nitrogen and sulfur atoms of the **FC4** sensor and Hg^{2+} will be able to facilitate the sensitive and selective binding.

The excellent sensitivity and selectivity of the sensor for Hg^{2+} in aqueous buffer solutions make it suitable for detecting permissible levels in drinking water and potentially useful for mercury detection in biological and environmental samples [101].

Poh Wei Cheah et al. developed a new fluorescent chemosensor (MEK) (Fig. 20) by conjugating rhodamine B hydrazide with methyl ethyl ketone. MEK enables 'naked-eye' detection with extraordinary selectivity and sensitivity for aluminum ions and Sn^{2+} ions, with limits of detection of 8.96 μM and 5.10 μM, consequently

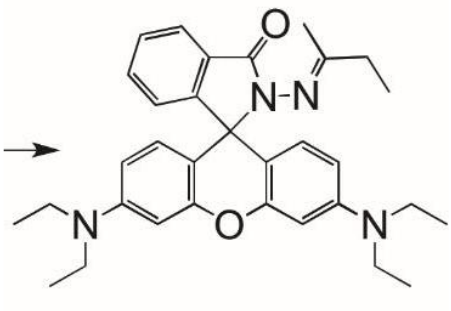

Fig. 20 Chemical Structure of Sensor MEK

MEK can identify the presence of both aluminum ions and tin ions because it can form colored coordination compounds with these metal ions. The MEK's amide carbonyl group participates in the complexation process with Sn^{2+} and Al^{3+}.

metal ions. MEK-coated sensor strips on filter sheets, combined with a basic UV light source, enable cost-effective, on-site 'naked-eye' detection of Al^{3+} and Sn^{2+} ions, offering a practical alternative to expensive equipment [102].

Jing-can Qin et al. developed a new fluorescent aluminum ions sensor, 8-hydroxyquinoline-7-aldehyde-(2'-methylquinoline-4'-formyl) hydrazone (L1) (Fig. 21), based on a quinoline compounds. The limit of detection was determined to be 5.2×10^{-6} M.

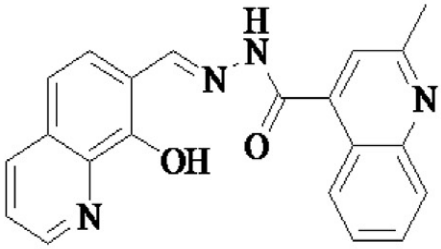

Fig. 21 Chemical Structure of Sensor L1

One maximal absorption band that was centered in the L1 absorption spectra is indicative of the quinoline group. The absorption bands gradually diminished and new, more intense absorption bands emerged when Al^{3+} was added. Additionally, two distinct isosbestic points emerged, indicating the existence of a novel complex in balance with the receptor. We suggested that the creation of a 1:2 ligand–metal complex, which inhibits the process of photo-induced electron transfer (PET), is the reason behind this occurrence. due to PET caused via lone pair of electrons coming from the nitrogen atom of C=N, the fluorescence band of HL was weak in the absence of aluminum ions. Following the addition of aluminum ions, the interaction between Al^{3+} and L1 prevented electrons from transferring from lone pair of electrons onto nitrogen of the C=N group to the quinoline ring, which led to a substantial increase in intensity of fluorescence. The L1 sensor has potential applications in detecting concentrations of micromolar of Al^{3+} in environmental and systems of biology [103].

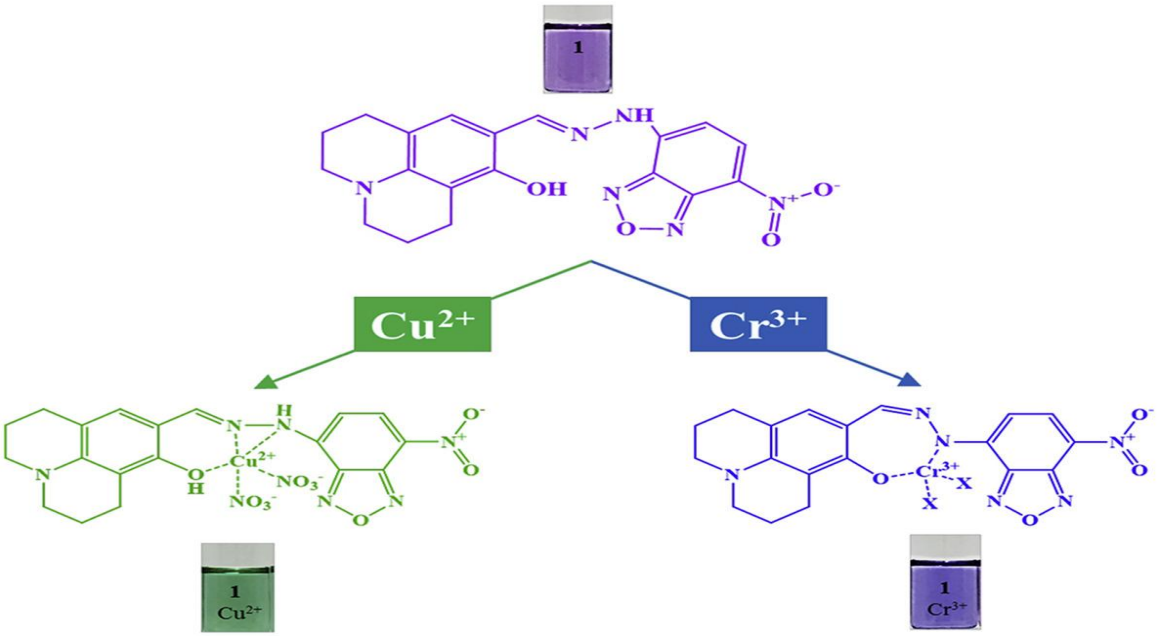

Scheme. 7 Schematic presentation of coordination of **NBD** with Cr^{3+} and Cu^{2+} ions.

Seong Youl Lee et al. created a new colorimetric chemosensor (1) based on NBD (7-nitrobenzo-2-oxa-1,3-diazolyl) and julolidine for detecting Cu^{2+} & Cr^{3+} ions. The limits of detection for Cr^{3+} and Cu^{2+} were calculated to be 0.59 μM and 0.36 μM, consequently.

Chemosensor 1 demonstrated practical applicability in detecting Cu^{2+} and Cr^{3+} (Scheme. 7) in water from tap, drinking water, and contaminated specimens with high recovery rates, suggesting its potential use in chemical and environmental analysis, including colorimetric test strips [104].

B. Kirthika Rani et al. developed a fluorogenic pyrene-amino mercapto thiadiazole (PYAMT) (Fig. 22) probe with a broad linear range (100 nM to 2.5 μM) and a limit of detection 0.35 nM, enabling extremely sensitive and selective Hg^{2+} estimation in water samples and live cells using bioimaging.

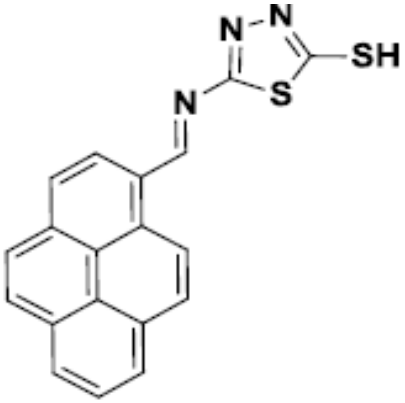

Fig. 22 Chemical Structure of Sensor PYAMT

The Hg^{2+} ion typically favors coordinating with ligands that have sulfur, oxygen, or nitrogen atoms. The mercaptothiadiazole unit of chemosensor (PYAMT) used as a chelator for mercury ions and the pyrene moiety as a receptor. The synthesized PYAMT exhibited a notable quenching in fluorescence upon complexation with diamagnetic Hg^{2+} ions. Because Hg^{2+} is a heavy ion, it increases spin-orbit coupling, which increases intersystem crossover and, as a result, quenches the probe's fluorescence intensity. The DFT investigations further demonstrated that the electron transfer from the pyrene unit to the metal ion of Hg^{2+} is what causes the quenching, which credited to the influence of heavy atoms.

PYAMT demonstrated effective bioimaging of Hg^{2+} in HeLa cells without significant toxicity and showed high recovery in detecting Hg^{2+} in natural water samples, making it suitable for real-world applications in biological and environmental analysis [105].

Jing-can Qin et al. created a basic fluorescent sensor, 7-(2',4'-dihydroxybenzylideneimino)-4-methyl coumarin (Fig. 23), with superior selectivity for aluminum ions and zinc ions. The limits of detection were determined to be 3.7×10^{-6} M for aluminum ions and 3.86×10^{-6} M for zinc ions.

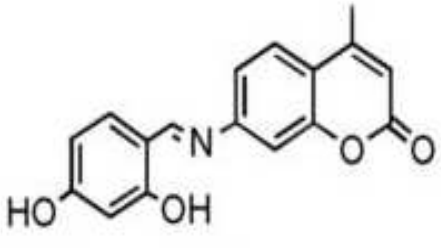

Fig. 23 Chemical Structure of 7-(2',4'-dihydroxybenzylideneimino)-4-methyl coumarin

The addition of Al^{3+} accelerated the Schiff-base breakdown, leading to significant fluorescence emission. For Zn^{2+}, the fluorescence was initially suppressed by the photoinduced electron transfer (PET) mechanism, facilitated by lone pair of electrons coming from the N atom of the –C=N group to coumarin. However, upon Zn^{2+} binding, chelation with the –C=N nitrogen inhibited the PET process, restoring fluorescence. Notably, this multifunctional fluorescent probe shows potential for detecting micromolar levels of Al^{3+} and Zn^{2+} and for environmental molecular recognition due to its low detection limit [106].

Zhimin Zhong et al. synthesized benzimidazo[2,1-a]benz[de]isoquinoline-7-one-13-(N-butylthioamide) (N4) using a thiocarbonyl-to-carbon conversion method induced by Hg^{2+}. Sensor N4 exhibited a rapid response time and high sensitivity, with a limit of detection 1.6×10^{-8} M for Hg^{2+}.

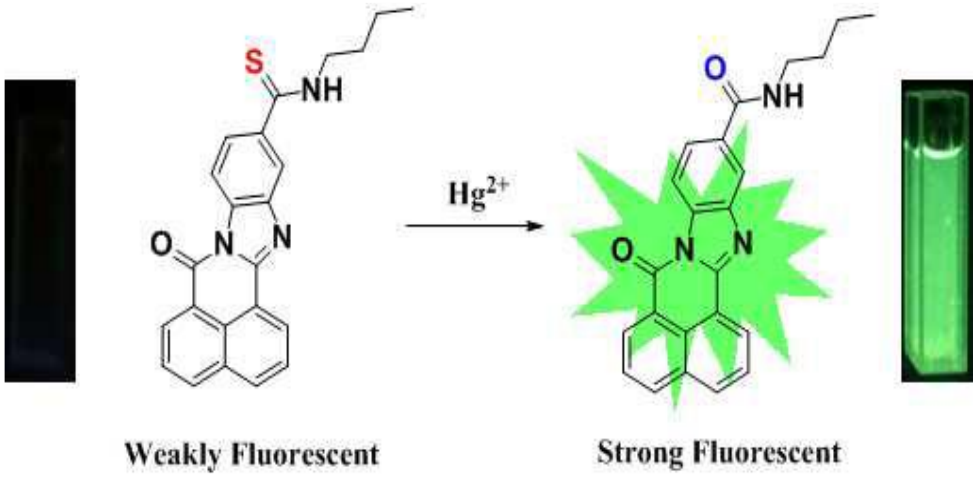

Scheme. 8 Schematic presentation of coordination of **N4** with Hg^{2+} ions.

The probe N4 responded to Hg^{2+} with a strong Stokes shift (red shift) and turn-on fluorescence emission (Scheme. 8). Since Hg^{2+} was a thiophilic metal ion, the mercury ions induced conversion of the thiocarbonyl group to the carbon one and subsequent elimination of the HgS should be the cause of the fluorescence amplification [107].

Ye Won Choi et al. synthesized a novel receptor (Sensor 1) by combining julolidine and 2-(aminomethyl)benzenamine. Sensor 1 exhibited a small limit of detection of 10.9 μM. Sensor 1 functions as a 'turn-on' chemosensor for Zn^{2+}, effectively distinguishing it from Cd^{2+}. The strong fluorescence enhancement for Zn^{2+} is attributed to the creation of a steady chelate complex, leading to a chelation-enhanced fluorescence (CHEF) effect. Normally, Sensor 1 is nearly non-fluorescent because of C=N isomerization in the excited state, but metal ion interaction restricts this process, significantly boosting fluorescence. These findings suggest that Sensor 1 provides a reliable system for selective Zn^{2+} detection in aqueous solutions, even when competitive metal ions are present, particularly Cd^{2+} [108].

Yongjie Ding et al. developed a novel quinoline derivative (QN) by combining 3-hydroxy-2-naphthoic hydrazide with quinoline-8-carboxaldehyde. QN functioned as a dual chemosensor, selectively recognizing Al^{3+} through fluorescence and detecting Fe^{2+} colorimetrically, with detection limits of 1.22×10^{-8} mol/ L for aluminum ions and 1.04×10^{-7} mol/ L for iron ions.

When QN was excited, a faint emission band was observed. This was credited to

the C = N isomerization and the photoinduced electron transfer (PET) that occurred because the non-bonding electrons were transferred to the huge π-conjugation system. Compound QN had a noteworthy selective response to the Al^{3+} ion in case of adding many various metal ions, resulting in an amplification of fluorescence. Conversely, in contrast to the free complex QN, the emission spectra that other metal ions showed little to no modification. The observed augmentation of fluorescence in the presence of aluminum ions may due to the chelation-enhanced fluorescence (CHEF) effect, which impeded the PET process and C=N isomerization of compound QN (Scheme. 9). The practical applicability of chemosensor QN was evaluated by analyzing real water specimens with varied quantity of aluminum ions and iron ions. The results confirmed its effectiveness in detecting these ions, emphasizing its opportunity for practical problems applications and future research of more efficient chemosensors [109].

Rasha M. Kamel et al. developed a fluorescent sensor, 5-(4-(dimethylamino)phenyl)-4-(2-(4-methoxy-3-methylphenyl)-2-oxoethyl)-1H-pyrazol-3(2H)-one (AAP), for the selective and sensitive detection of Fe^{3+} in industrial wastewater. The sensor showed a linear fluorescence intensity response within 0–50 μmol L^{-1} and exhibited minimal interference effects. The detection and quantitation limits were determined to be 1.59 nmol/ L and 5.31 nmol/ L,

correspondingly, with satisfactory results in real wastewater applications. The **AAP** sensor is poorly fluorescent due to its highly electron-donating group (N–N dimethylamino) conjugated to an electron-withdrawing group (carbonyl oxygen) and excited-state intramolecular proton-transfer (ESIPT) effect caused by lactam-lactim tautomerism. The chelation of iron ions with two carbonyl oxygen of the AAP sensor reduces the ESIPT effect, which enhances fluorescence. Additionally, chelation with iron ions causes rigidity in the resultant compound, which increases the chelation enhanced fluorescence (CHEF) effect. An AAP sensor test strip was developed for practical Fe^{3+} detection in real water samples [110].

In summary, small organic molecule-based sensors demonstrate high potential for the selective and sensitive detection of various pollutants, particularly heavy metal ions. To provide a clear overview of the current progress in this field, a summarized comparison of representative sensors including their target ions and detection limits is presented in Table 1.

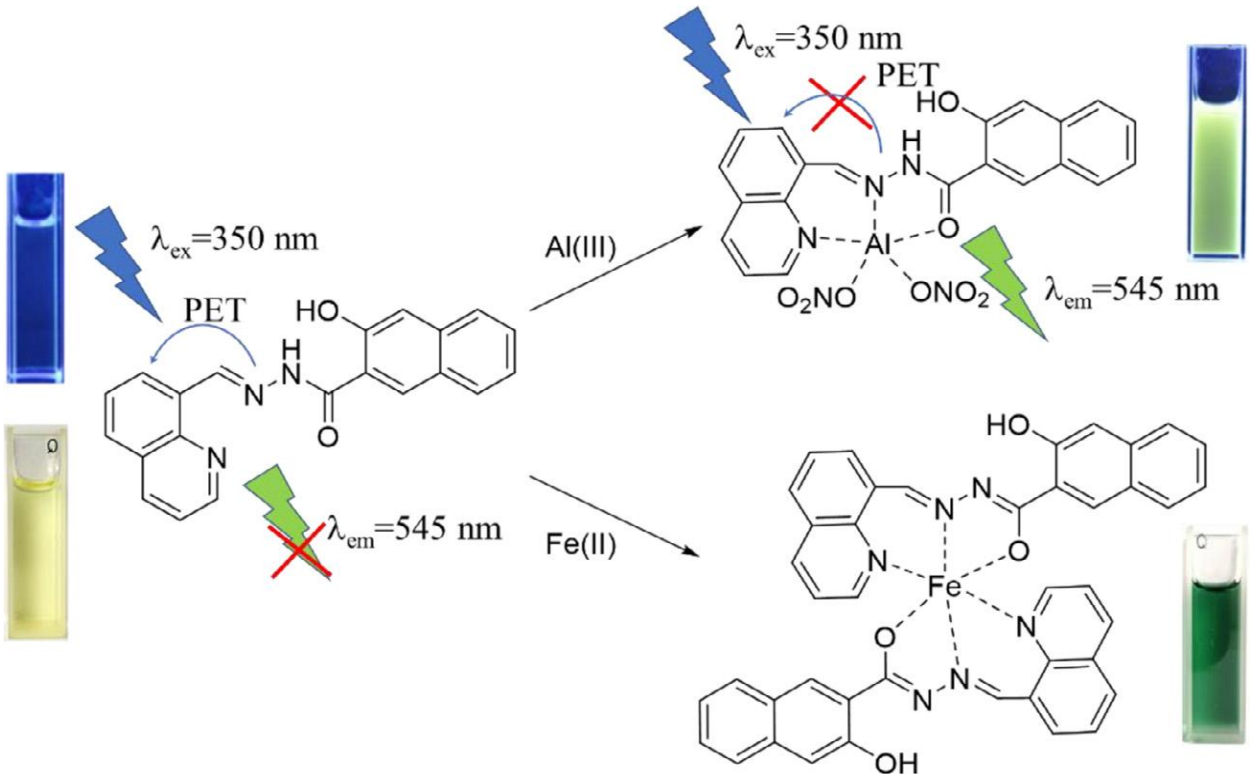

Scheme. 9 Schematic presentation of coordination of **QN** with Fe^{2+} and Al^{3+} ions.

Table1: Summary of representative small organic molecule-based sensors for the detection of heavy metal ions, including their target ions and corresponding detection limits.

Sensor	Target Ions	Limit of Detection (LOD)	Ref.
QLBM sensor	Cu^{2+}, Fe^{3+}	1.35×10^{-7} M (Cu^{2+}) 1.24×10^{-7} M (Fe^{3+})	[76]
APSS, APTS sensors	Fe^{3+}	45.9 nM (APSS)	[77]
Naphthalene-based Acetohydrazide Derivative	Al^{3+}	0.34 mmol/L	[78]
Sensor 1O	Zn^{2+}, Al^{3+}	2.97×10^{-9} mol/L	[79]
BF	Al^{3+}	1.04 mmol L^{-1}	[80]
HL	Mg^{2+}, Zn^{2+}	3.07×10^{-7} M (Mg^{2+}) 2.97×10^{-8} M (Zn^{2+})	[81]
NT	Al^{3+}	1.1×10^{-7} M	[82]
L	Hg^{2+}	1.1×10^{-6} M	[83]
1O	Cu^{2+}	Not specified	[84]

Sensor	Target Ions	Limit of Detection (LOD)	Ref.
PYMH	Zn^{2+}	5.1 nM	[85]
H_4L	Cr^{3+}, Al^{3+}	4.87×10^{-7} M	[86]
S	Al^{3+}	4.55×10^{-11} M	[87]
L	Zn^{2+}, Cu^{2+}	45 nM (Zn^{2+}) 17 nM (Cu^{2+})	[88]
1O	Al^{3+}, Zn^{2+}	8.31×10^{-8} mol/L (Al^{3+}) 3.33×10^{-7} mol/L (Zn^{2+})	[89]
WS1	Cu^{2+}	4.32×10^{-8} M	[90]
H_2L	Zn^{2+}, Al^{3+}, F^-	2.24×10^{-7} M (Zn^{2+}) 4.1×10^{-8} M (Al^{3+}) 3.7×10^{-8} M (F^-)	[91]
4-amino-1,8-naphthalimide-conjugated polyamidoamine dendrimer	Ag^+	Detection range: 0.3×10^{-4} - 4.8×10^{-4} M	[92]
RHCS-NH_2	Ca^{2+}, Zn^{2+}	0.10 nM (Ca^{2+}) & 0.14 nM (Zn^{2+})	[93]
CTS (94)	Zn^{2+}	5.03×10^{-7} M	[94]
H2L (95)	Zn^{2+}, Al^{3+}	5.86×10^{-6} mol/L (Al^{3+}) 1.81×10^{-6} mol/L (Zn^{2+})	[95]
isatin-3-(7'-methoxychromone-3'-methylidene) hydrazone	Mg^{2+}	5.16×10^{-7} M	[96]
R	Cu^{2+}, Zn^{2+}	17.3 ppb (Cu^{2+}) 16.5 ppb (Zn^{2+})	[97]
H_3SAL-NH	Zn^{2+}, Al^{3+}	3.1 nM (Zn^{2+}) 0.92 nM (Al^{3+})	[98]
B3a, B3b, B3c	Hg^{2+}, Cr^{3+}, Fe^{3}	Not specified	[99]
L	Al^{3+}	8.2×10^{-7} M	[100]
FC4	Hg^{2+}	7.38×10^{-9} M	[101]
MEK	Al^{3+}, Sn^{2+}	8.96 µM (Al^{3+}) 5.10 µM (Sn^{2+})	[102]
L1	Al^{3+}	5.2×10^{-6} M	[103]
1	Cu^{2+}, Cr^{3+}	0.36 µM (Cu^{2+}) 0.59 µM (Cr^{3+})	[104]
PYAMT	Hg^{2+}	0.35 nM	[105]
(2',4'-dihydroxybenzylideneimino)-4-methyl coumarin (106)	Al^{3+}, Zn^{2+}	3.7×10^{-6} M (Al^{3+}) 3.86×10^{-6} M (Zn^{2+})	[106]
N4	Hg^{2+}	1.6×10^{-8} M	[107]
Sensor 1	Zn^{2+}	10.9 µM	[108]
QN	Al^{3+}, Fe^{2+}	1.22×10^{-8} M (Al^{3+}) 1.04×10^{-7} M (Fe^{2+})	[109]
AAP	Fe^{3+}	1.59 nM	[110]

Conclusion

Despite remarkable progress in the development of heavy metal detection technologies, key challenges continue to limit their widespread deployment. Conventional techniques, while highly sensitive, are often expensive, complex, and impractical for on-site use. Emerging optical and electrochemical methods offer improved portability but still face issues such as matrix interference and limited sensitivity or selectivity. Fluorescent sensors, particularly those based on small organic molecules, show great promise due to their adaptability, high sensitivity, and potential for miniaturization; however, their performance in

real-world matrices and integration into practical devices remain areas for further advancement. From environmental and industrial monitoring to clinical diagnostics, food safety, and smart city integration, advanced sensing systems have the potential to provide rapid, reliable, and cost-effective solutions for heavy metal contamination. As research continues to address current limitations—especially in terms of multi-analyte detection, real-time monitoring, and eco-friendly design—the future holds great promise for achieving more accessible and effective heavy metal sensing platforms that protect both public health and the environment.

References

1. Abd Elnabi, M.K., Elkaliny, N.E., Elyazied, M.M., Azab, S.H., Elkhalifa, S.A., Elmasry, S., Mouhamed, M.S., Shalamesh, E.M., Alhorieny, N.A., Abd Elaty, A.E. and Elgendy, I.M. "Toxicity of Heavy Metals and Recent Advances in Their Removal: A Review." *Toxics* 11(7) (2023) 580. https://doi.org/10.3390/toxics11070580.
2. Appannagari, R. R. Environmental pollution causes and consequences: a study. *North Asian International Research Journal of Social Science & Humanities*, *3*(8), (2017) 151-161.
3. Ajibade, F.O., Adelodun, B., Lasisi, K.H., Fadare, O.O., Ajibade, T.F., Nwogwu, N.A., Sulaymon, I.D., Ugya, A.Y., Wang, H.C. and Wang, A. "Environmental Pollution and Their Socioeconomic Impacts." *Microbe Mediated Remediation of Environmental Contaminants*, (2021) 321-354. http://doi.org/10.1016/b978-0-12-821199-1.00025-0
4. Khan, I. U., S. S. Qi, F. Gul, S. Manan, J. K. Rono, M. Naz, X. N. Shi, H. Zhang, Z. C. Dai, and D. L. Du. "A Green Approach Used for Heavy Metals 'Phytoremediation' Via Invasive Plant Species to Mitigate Environmental Pollution: A Review." *Plants* (Basel) 12 (4) (2023) 725. https://dx.doi.org/10.3390/plants12040725.
5. Timothy, N.A. and Williams, E.T. "Environmental Pollution by Heavy Metal: An Overview." *International Journal of Environmental Chemistry* 3 (2) (2019) 72-82.https://dx.doi.org/10.11648/j.ijec.20190302.14.
6. Xu, H., Y. Jia, Z. Sun, J. Su, Q. S. Liu, Q. Zhou, and G. Jiang. "Environmental Pollution, a Hidden Culprit for Health Issues." *Eco Environ Health* 1(1) (2022): 31-45. https://dx.doi.org/10.1016/j.eehl.2022.04.003.
7. Singh, V., N. Singh, S. N. Rai, A. Kumar, A. K. Singh, M. P. Singh, A. Sahoo, S. Shekhar, E. Vamanu, and V. Mishra. "Heavy Metal Contamination in the Aquatic Ecosystem: Toxicity and Its Remediation Using Eco-Friendly Approaches." *Toxics* 11 (2) (2023) 147. https://dx.doi.org/10.3390/toxics11020147.
8. Zhu, L., Husny, Z.J.B.M., Samsudin, N.A., Xu, H. and Han, C. "Deep Learning Method for Minimizing Water Pollution and Air Pollution in Urban Environment." *Urban Climate* 49 (2023) 101486. https://dx.doi.org/10.1016/j.uclim.2023.101486.
9. Aziz, K.H.H., Mustafa, F.S., Omer, K.M., Hama, S., Hamarawf, R.F. and Rahman, K.O. "Heavy Metal Pollution in the Aquatic Environment: Efficient and Low-Cost Removal Approaches to Eliminate Their Toxicity: A Review." *RSC Advances*, 13 (26) (2023) 17595-610. https://dx.doi.org/10.1039/d3ra00723e.
10. Zahra, N., Kalim, I., Mahmood, M. and Naeem, N. "Perilous Effects of Heavy Metals Contamination on Human Health." *Pakistan Journal of Analytical & Environmental Chemistry* 18 (1) (2017) 1-17. https://dx.doi.org/10.21743/pjaec/2017.06.01.
11. Khasanova, S.S. and Saydulgerieva, M.A. "Environmental Pollution and Implementation of Sustainable Development Goals." *BIO Web of Conferences* 82 EDP Sciences (2024) 06007. https://dx.doi.org/10.1051/bioconf/20248206007.
12. Zhang, P., Yang, M., Lan, J., Huang, Y., Zhang, J., Huang, S., Yang, Y. and Ru, J. "Water Quality Degradation Due to Heavy Metal Contamination: Health Impacts and Eco-Friendly Approaches for Heavy Metal Remediation." *Toxics* 11 (10) (2023) 828. https://dx.doi.org/10.3390/toxics11100828.
13. Witkowska, D., Słowik, J. and Chilicka, K. "Heavy Metals and Human Health: Possible Exposure Pathways and the Competition for Protein Binding Sites." *Molecules* 26 (19) (2021) 6060. https://dx.doi.org/10.3390/molecules26196060.
14. Haidar, Z., Fatema, K., Shoily, S.S. and Sajib, A.A. "Disease-Associated Metabolic Pathways Affected by Heavy Metals and Metalloid." *Toxicology Reports* 10 (2023) 554-570. https://dx.doi.org/10.1016/j.toxrep.2023.04.010.
15. Coradduzza, D., Congiargiu, A., Azara, E., Mammani, I.M.A., De Miglio, M.R., Zinellu, A., Carru, C. and Medici, S. "Heavy Metals in Biological Samples of Cancer Patients: A Systematic Literature Review." *Biometals* 37 (4) (2024) 803-817. https://dx.doi.org/10.1007/s10534-024-00583-4.
16. Boumba, V.A., Ziavrou, K.S. and Vougiouklakis, T. "Hair as a Biological Indicator of Drug Use, Drug Abuse or Chronic Exposure to Environmental Toxicants." *International Journal of Toxicology*, *25*(3) (2006) 143-163. https://dx.doi.org/10.1080/10915810600683028.
17. Peter, O.O., Eneji, I.S. and Sha'Ato, R. "Analysis of Heavy Metals in Human Hair Using Atomic Absorption Spectrometry (AAS)." *American Journal of Analytical Chemistry* 03 (11) (2012) 770-773. https://dx.doi.org/10.4236/ajac.2012.311102.
18. Afridi, H.I., Kazi, T.G., Kazi, N., Baig, J.A., Jamali, M.K., Arain, M.B., Sarfraz, R.A., Sheikh, H.U.R., Kandhro, G.A. and Shah, A.Q. "Status of Essential Trace Metals in Biological Samples of Diabetic Mother and Their Neonates." *Archives of Gynecology and Obstetrics* 280 (3) (2009) 415-423. https://dx.doi.org/10.1007/s00404-009-0955-x.
19. Sikdar, S. and Kundu, M. "A Review on Detection and Abatement of Heavy Metals." *ChemBioEng Reviews* 5 (1) (2017) 18-29. https://dx.doi.org/10.1002/cben.201700005
20. Ali, A.H. "High-Performance Liquid Chromatography (Hplc): A Review." *Annals of Advances in Chemistry* 6 (1) (2022) 010-20. https://dx.doi.org/10.29328/journal.aac.1001026
21. Siddique, I.M. "Unveiling the Power of High-Performance Liquid Chromatography: Techniques, Applications, and Innovations. " *European Journal of Advances in Engineering and Technology* 8 (9) (2021) 79-84. http://dx.doi.org/10.2139/ssrn.4883906
22. Bulska, E. and Ruszczyńska, A. "Analytical Techniques for Trace Element Determination." *Physical Sciences Reviews* 2 (5) (2017) 20178002. https://dx.doi.org/10.1515/psr-2017-8002
23. Ohtsu, N., Ashino, T., Kimura, H., Takada, K. and Hanawa, T. "Investigation for Analytical Procedure for Determination of Trace Metallic Ions in Simulated Body Fluids by Inductively Coupled Plasma Atomic Emission Spectrometry (Icp-Aes)." *Journal of Materials Science: Materials in Medicine* 18 (3) (2007) 429-33. https://dx.doi.org/10.1007/s10856-007-2001-5
24. Nomngongo, P. N., Ngila, J. C., Msagati, T.A.M. and Moodley, B. "Preconcentration of Trace Multi-Elements in Water Samples Using Dowex 50w-X8 and Chelex-100 Resins Prior to Their Determination Using Inductively Coupled Plasma Atomic Emission Spectrometry (Icp-Oes)." *Physics and Chemistry of the Earth, Parts A/B/C* 66 (2013) 83-88. https://dx.doi.org/10.1016/j.pce.2013.08.007
25. García-Otero, N., Barciela-Alonso, Mª. C., Domínguez-González, R., Herbello-Hermelo, P., Moreda-Piñeiro, A. and Bermejo-Barrera, P. "Evaluation of Offgel Electrophoresis, Electrothermal Atomic Absorption Spectroscopy and Inductively

Coupled Plasma Optical Emission Spectroscopy for Trace Metal Analysis in Marine Plankton Protein." *Microchemical Journal* 119 (2015) 51-57. https://dx.doi.org/10.1016/j.microc.2014.11.001
26. Barbaste, M., Robinson, K., Guilfoyle, S., Medina, B. and Lobinski, R. "Precise Determination of the Strontium Isotope Ratios in Wine by Inductively Coupled Plasma Sector Field Multicollector Mass Spectrometry (Icp-Sf-Mc-Ms)." *Journal of Analytical Atomic Spectrometry* 17(2) (2002) 135-37. https://dx.doi.org/10.1039/b109559p
27. Moens, L. "Applications of mass spectrometry in the trace element analysis of biological materials. " *Fresenius Journal of Analytical Chemistry* 359 (1997) 309–316. https://doi.org/10.1007/s002160050579
28. Yang, L., Zhang, M., Lin, S., Chen, D. and Zheng, M. "Minor and Trace Element Analysis in Breast Milk Using Inductively Coupled Plasma Mass Spectrometry (Icp-Ms)." *Microchimica Acta* 142 (1-2) (2003) 85-88. https://dx.doi.org/10.1007/s00604-003-0003-7
29. Ammann, A. A. "Inductively Coupled Plasma Mass Spectrometry (Icp Ms): A Versatile Tool." *Journal of Mass Spectrometry* 42(4) (2007) 419-27. https://dx.doi.org/10.1002/jms.1206
30. Becker, J. S. "Trace and Ultratrace Analysis in Liquids by Atomic Spectrometry." *TrAC Trends in Analytical Chemistry* 24 (3) (2005) 243-54. https://dx.doi.org/10.1016/j.trac.2004.12.003
31. Wojciechowski, M., Krata, A. and Bulska,E. "Detremination of Mercury Isotopic Profile by Inductively Coupled Plasma Mass Spectrometry: Possibilities and Limitations "*Chemia. Analityczna. (Warsaw)* 53(6) (2008) 797-808.
32. Hattendorf, B. and Günther, D. "Characteristics and Capabilities of an Icp-Ms with a Dynamic Reaction Cell for Dry Aerosols and Laser Ablation." *Journal of Analytical Atomic Spectrometry* 15 (9) (2000) 1125-31. https://dx.doi.org/10.1039/b001677m
33. De Boer, J. L.M., Ritsema, R., Piso, S., Staden, H.V. and Den Beld,W.V. "Practical and Quality-Control Aspects of Multi-Element Analysis with Quadrupole Icp-Ms with Special Attention to Urine and Whole Blood." *Analytical and Bioanalytical Chemisitry* 379 (5-6) (2004) 872-80. https://dx.doi.org/10.1007/s00216-004-2654-6
34. Pujol, L., Evrard, D., Groenen-Serrano, K., Freyssinier, M., Ruffien-Cizsak, A. and Gros, P. "Electrochemical Sensors and Devices for Heavy Metals Assay in Water: The French Groups' Contribution." *Frontiers in Chemistry* 2 (2014) 19. https://dx.doi.org/10.3389/fchem.2014.00019
35. Fan, L., Chen, J., Zhu, S., Wang, M. and Xu,G. "Determination of Cd2+ and Pb2+ on Glassy Carbon Electrode Modified by Electrochemical Reduction of Aromatic Diazonium Salts." *Electrochemistry Communications* 11 (9) (2009) 1823-25. https://dx.doi.org/10.1016/j.elecom.2009.07.026
36. Aragay, G. and Merkoçi, A. "Nanomaterials Application in Electrochemical Detection of Heavy Metals." *Electrochimica Acta* 84 (2012) 49-61. https://dx.doi.org/10.1016/j.electacta.2012.04.044
37. Lu, Y., Liang, X., Niyungeko, C., Zhou, J., Xu, J. and Tian, G. "A Review of the Identification and Detection of Heavy Metal Ions in the Environment by Voltammetry." *Talanta* 178 (2018) 324-38. https://dx.doi.org/10.1016/j.talanta.2017.08.033
38. Silva, J. J., Paim, L.L. and Stradiotto, N.R. "Simultaneous Determination of Iron and Copper in Ethanol Fuel Using Nafion /Carbon Nanotubes Electrode." *Electroanalysis* 26(8) (2014) 1794-1800. https://dx.doi.org/10.1002/elan.201400136
39. Devi, N. R., Sasidharan, M. and Sundramoorthy, A.K. "Gold Nanoparticles-Thiol-Functionalized Reduced Graphene Oxide Coated Electrochemical Sensor System for Selective Detection of Mercury Ion." *Journal of The Electrochemical Society* 165 (8) (2018) B3046-B53. https://dx.doi.org/10.1149/2.0081808jes
40. Xia, F., Zhang, X., Zhou, C., Sun, D., Dong, Y. and Liu., Z. "Simultaneous Determination of Copper, Lead, and Cadmium at Hexagonal Mesoporous Silica Immobilized Quercetin Modified Carbon Paste Electrode." *Journal of Automated Methods and Management in Chemistry* 2010 (2010) 824197. https://doi.org/10.1155/2010/824197
41. Pei, X., Kang, W., Yue, W., Bange, A., Heineman, W. R. and Papautsky, I. "Disposable Copper-Based Electrochemical Sensor for Anodic Stripping Voltammetry." *Analytical Chemistry* 86 (10) (2014) 4893-900. https://doi.org/10.1021/ac500277j
42. Yao, X. Z., Guo, Z. Yuan, Q. H., Liu, Z. G., Liu, J. H. and Huang, X. J. "Exploiting Differential Electrochemical Stripping Behaviors of Fe3o4 Nanocrystals toward Heavy Metal Ions by Crystal Cutting." *ACS Applied Materials & Interfaces* 6 (15) (2014) 12203-13. https://dx.doi.org/10.1021/am501617a
43. Arduini, F., Majorani, C., Amine, A., Moscone, D. and Palleschi,G. "Hg2+ Detection by Measuring Thiol Groups with a Highly Sensitive Screen-Printed Electrode Modified with a Nanostructured Carbon Black Film." *Electrochimica Acta* 56 (11) (2011) 4209-15. https://doi.org/10.1016/j.electacta.2011.01.094
44. Salinas, G. and Frontana-Uribe, B.A.. "Electrochemical Analysis of Heavy Metal Ions Using Conducting Polymer Interfaces." *Electrochem* 3 (3) (2022) 492-506. https://doi.org/10.3390/electrochem3030034
45. Choi, S. M., Kim, D. M., Jung, O. S. and Shim, Y. B. "A Disposable Chronocoulometric Sensor for Heavy Metal Ions Using a Diaminoterthiophene-Modified Electrode Doped with Graphene Oxide." *Analytica Chimica Acta* 892 (2015) 77-84. https://dx.doi.org/10.1016/j.aca.2015.08.037
46. Venkataprasad, G., Reddy, T.M., Shaikshavali, P. and Gopal,P. "A Novel Electrochemical Sensor Based on Multi-Walled Carbon Nanotubes/Poly (L-Methionine) for the Investigation of 5-Nitroindazole: A Voltammetric Study." *Analytical Chemistry Letters* 8 (4) (2018) 457-74. https://doi.org/10.1080/22297928.2018.1479304
47. Jin, M., Yuan, H., Liu, B., Peng, J., Xu, L. and Yang, D. "Review of the Distribution and Detection Methods of Heavy Metals in the Environment." *Analytical Methods* 12 (48) (2020) 5747-66. https://doi.org/10.1039/D0AY01577F
48. Butler, O. T., Cook, J.M., Harrington, C.F., Hill, S.J., Rieuwerts, J and Miles,D.L. "Atomic Spectrometry Update. Environmental Analysis." *Journal of Analytical Atomic Spectrometry* 22(2) (2007) 217-243. https://doi.org/10.1039/B516025C
49. Elik, A., Demirbas, A., and Altunay, N. "Analysis of Zinc and Chromium in Grain Samples Using Ionic Liquid-Based Ultrasound-Assisted Microextraction Followed by Flame-Aas after Microwave Digestion." *Biological Trace Element Research* 198 (2) (2020): 697-706. https://dx.doi.org/10.1007/s12011-020-02071-5
50. Vinogradova, N., Glukhov, A., Chaplygin, V., Kumar, P., Mandzhieva, S., Minkina, T., and Rajput,V.D. "The Content of Heavy Metals in Medicinal Plants in Various Environmental Conditions: A Review." *Horticulturae* 9 (2) (2023) 239. https://doi.org/10.3390/horticulturae9020239
51. Yuan, X., Chapman, R. L. and Wu, Z. "Analytical Methods for Heavy Metals in Herbal Medicines." *Phytochemical Analysis* 22 (3) (2011) 189-198. https://doi.org/10.1002/pca.1287
52. Chuang, I.C., Chen, K.S., Huang, Y.L., Lee, P.N. and Lin, T.H. Determination of trace elements in some natural drugs by atomic absorption spectrometry. *Biological Trace Element Research* 76 (2000) 235-244. https://doi.org/10.1385/BTER:76:3:235
53. Biata, N. R., Dimpe, K.M., Ramontja, J., Mketo, N. and Nomngongo,P.N. "Determination of Thallium in Water Samples

Using Inductively Coupled Plasma Optical Emission Spectrometry (Icp-Oes) after Ultrasonic Assisted-Dispersive Solid Phase Microextraction." *Microchemical Journal* 137 (2018) 214-22. https://doi.org/10.1016/j.microc.2017.10.020

54. Kearton, B., Mattley, Y. Sparking new applications. *Nature Photon* 2 (2008) 537–540. https://doi.org/10.1038/nphoton.2008.173

55. Galbacs, G. "A Critical Review of Recent Progress in Analytical Laser-Induced Breakdown Spectroscopy." *Analytical & Bioanalytical Chemistry* 407(25) (2015) 7537-62. https://doi.org/10.1007/s00216-015-8855-3

56. Lee, Y., Oh, S. W., and Han, S.H. "Laser-Induced Breakdown Spectroscopy (Libs) of Heavy Metal Ions at the Sub-Parts Per Million Level in Water." *Applied Spectroscopy* 66 (12) (2012) 1385-96. https://doi.org/10.1366/12-06639R

57. Randall, D. W., Hayes, R.T. and Wong, P.A. "A Simple Laser Induced Breakdown Spectroscopy (Libs) System for Use at Multiple Levels in the Undergraduate Chemistry Curriculum." *Journal of Chemical Education* 90 (4) (2013) 456-62. https://doi.org/10.1021/ed300350a

58. Guo, Y.M., Guo, L.B., Li, J.M., Liu, H.D., Zhu, Z.H., Li, X.Y., Lu, Y.F.and Zeng,X.Y. "Research Progress in Asia on Methods of Processing Laser-Induced Breakdown Spectroscopy Data." *Frontiers of Physics* 11(5) (2016) 114212.https://doi.org/10.1007/s11467-016-0604-3

59. Jantzi, S. C., Ros, V.M., Trichard, F., Markushin, Y., Melikechi, N., and De Giacomo, A. "Sample Treatment and Preparation for Laser-Induced Breakdown Spectroscopy." *Spectrochimica Acta Part B: Atomic Spectroscopy* 115 (2016) 52-63. https://doi.org/10.1016/j.sab.2015.11.002

60. Byers, H. L., McHenry, L. J. and Grundl, T. J. "Xrf Techniques to Quantify Heavy Metals in Vegetables at Low Detection Limits." *Food Chemistry: X* 1 (2019) 100001. https://doi.org/10.1016/j.fochx.2018.100001

61. Feng, X., Zhang, H. and Yu, P. "X-Ray Fluorescence Application in Food, Feed, and Agricultural Science: A Critical Review." *Critical Reviews in Food Science and Nutrition* 61 (14) (2021) 2340-50. https://dx.doi.org/10.1080/10408398.2020.1776677

62. Marguí, E., Queralt, I. and Hidalgo, M. "Application of X-Ray Fluorescence Spectrometry to Determination and Quantitation of Metals in Vegetal Material." *TrAC Trends in Analytical Chemistry* 28(3) (2009) 362-72. https://dx.doi.org/10.1016/j.trac.2008.11.011

63. Strange, R. W. and Feiters, M. C. "Biological X-Ray Absorption Spectroscopy (Bioxas): A Valuable Tool for the Study of Trace Elements in the Life Sciences." *Current Opinion in Structural Biology* 18 (5) (2008) 609-16. https://dx.doi.org/10.1016/j.sbi.2008.06.002

64. Maratta, A., Vázquez, S., López, A., Augusto, M. and Pacheco, P. H. "Lead Preconcentration by Solid Phase Extraction Using Oxidized Carbon Xerogel and Spectrophotometric Determination with Dithizone." *Microchemical Journal* 128 (2016) 166-71. https://dx.doi.org/10.1016/j.microc.2016.04.017

65. Rajabi, H. R. and Razmpour, S. "Synthesis, Characterization and Application of Ion Imprinted Polymeric Nanobeads for Highly Selective Preconcentration and Spectrophotometric Determination of Ni^{2+} Ion in Water Samples." *Spectrochimica Acta Part A: Molecular and Biomolecular Spectroscopy* 153 (2016) 45-52. https://dx.doi.org/10.1016/j.saa.2015.08.010

66. Lace, A., Ryan, D., Bowkett, M. and Cleary, J. "Chromium Monitoring in Water by Colorimetry Using Optimised 1,5-Diphenylcarbazide Method." *International Journal of Environmental Research and Public Health* 16 (10) (2019) 1803. https://dx.doi.org/10.3390/ijerph16101803.

67. Richter, M. M. "Electrochemiluminescence (ECL) " *Chemical Reviews* 104 (6) (2004) 3003-3036. https://doi.org/10.1021/cr020373d

68. Valenti, G., Fiorani, A., Li, H., Sojic, N. and Paolucci, F. "Essential Role of Electrode Materials in Electrochemiluminescence Applications." *ChemElectroChem* 3 (12) (2016) 1990-97. https://dx.doi.org/10.1002/celc.201600602.

69. Bertoncello, P.P. and Ugo, P. "Recent Advances in Electrochemiluminescence with Quantum Dots and Arrays of Nanoelectrodes." *ChemElectroChem* 4 (7) (2017) 1663-76. https://dx.doi.org/10.1002/celc.201700201.

70. Fiorani, A., Merino, J.P., Zanut, A., Criado, A., Valenti, G., Prato, M. and Paolucci,F. "Advanced Carbon Nanomaterials for Electrochemiluminescent Biosensor Applications." *Current Opinion in Electrochemistry* 16 (2019) 66-74. https://dx.doi.org/10.1016/j.coelec.2019.04.018.

71. Pedrero, M., Campuzano, S. and Pingarron, J. M. "Quantum Dots as Components of Electrochemical Sensing Platforms for the Detection of Environmental and Food Pollutants: A Review." *Journal of AOAC International* 100 (4) (2017) 950-61. https://dx.doi.org/10.5740/jaoacint.17-0169.

72. Sun, J., Sun, H. and Liang, Z. "Nanomaterials in Electrochemiluminescence Sensors." *ChemElectroChem* 4 (7) (2017) 1651-62. https://dx.doi.org/10.1002/celc.201600920.

73. Chen, X., Wang, W. and Li, B. "Novel Nanomaterials for the Fabrication of Electrochemiluminescent Sensors." In *Novel Nanomaterials for Biomedical, Environmental and Energy Applications* (2019) 189-214. https://doi.org/10.1016/B978-0-12-814497-8.00006-0

74. Ahluwalia, V.K." Instrumental Method of Chemical Analysis." Springer Cham (2017). https: //doi.org/10.1007/978-3-031-38355-7.

75. Mukherjee, A.G., Renu, K., Gopalakrishnan, A.V., Veeraraghavan, V.P., Vinayagam, S., Paz-Montelongo, S., Dey, A., Vellingiri, B., George, A., Madhyastha, H. and Ganesan, R. "Heavy Metal and Metalloid Contamination in Food and Emerging Technologies for Its Detection." *Sustainability* 15 (2) (2023) 1195. https://dx.doi.org/10.3390/su15021195.

76. Zhang, B., Liu, H., Wu, F., Hao, G. Chen, Y. Tan, C. Tan, Y. and Jiang, Y. "A Dual-Response Quinoline-Based Fluorescent Sensor for the Detection of Copper (II) and Iron (III) Ions in Aqueous Medium." *Sensors and Actuators B: Chemical* 243 (2017) 765-74. https://dx.doi.org/10.1016/j.snb.2016.12.067

77. Chaudhari, A., Patil, O. Janwadkar, H. Karpe, A. Kumar, V. Chetti, P. Patil, B. M., Ganesan, G. and Chaskar,A. "Ultra-Selective Pyrene-Based Fluorescent Sensor for Detection of Fe^{+3} in Neat Aqueous Medium." *Journal of Photochemistry and Photobiology A: Chemistry* 456 (2024).115874. https://dx.doi.org/10.1016/j.jphotochem.2024.115874.

78. Tümay, S. O., Şenocak, A. and Mermer,A. "A "Turn-on" Small Molecule Fluorescent Sensor for the Determination of $Al3^{+}$ Ion in Real Samples: Theoretical Calculations, and Photophysical and Electrochemical Properties." *New Journal of Chemistry* 45 (39) (2021) 18400-18411. https://dx.doi.org/10.1039/d1nj03462f.

79. Liang, Y., Diao, L. Wang, R., Wang, N. and Pu, S. "A Bifunctional Probe for Al^{3+} and Zn^{2+} Based on Diarylethene with an Ethylimidazo[2,1-B]Thiazole-6-Hydrazide Unit." *Tetrahedron Letters* 60 (2) (2019) 106-112. https://dx.doi.org/10.1016/j.tetlet.2018.11.066.

80. Zhang, Y., Fang, Y., Xu, N. Z., Zhang, M. Q., Wu, G. Z. and Yao, C. "A Colorimetric and Ratiometric Fluorescent Chemosensor Based on Furan-Pyrene for Selective and Sensitive Sensing $Al3^{+}$." *Chinese Chemical Letters* 27 (11) (2016) 1673-78. https://dx.doi.org/10.1016/j.cclet.2016.04.011.

81. Wang, Y., Wang, Z. G., Song, X. Q., Chen, Q., Tian, H., Xie, C. Z., Li, Q. Z. and Xu, J. Y. "A Dual Functional Turn-on Non-

Toxic Chemosensor for Highly Selective and Sensitive Visual Detection of Mg^{2+} and Zn^{2+}: The Solvent-Controlled Recognition Effect and Bio-Imaging Application." *Analyst* 144 (13) (2019) 4024-32. https://dx.doi.org/10.1039/c9an00583h.
82. Wang, Q.M., Gao, W., Tang, X.H., Liu, Y. and Li,Y. "A Fluorescence Turn-on Sensor for Aluminum Ion by a Naphthaldehyde Derivative." *Journal of Molecular Structure* 1109 (2016) 127-30. https://dx.doi.org/10.1016/j.molstruc.2015.12.076.
83. Feng, W., Xia, Q., Zhou, H., Ni, Y., Wang, L., Jing, S., Li, L. and Ji, W. "A Fluorescent Probe Based Upon Anthrancene-Dopamine Thioether for Imaging Hg^{2+} Ions in Living Cells." *Talanta* 167 (2017) 681-87. https://dx.doi.org/10.1016/j.talanta.2017.03.012.
84. Ma, L., Liu, G., Pu, S., Ding, H., and Li,G. "A Highly Selective Fluorescent Chemosensor for Cu^{2+} Based on a New Diarylethene with Triazole-Linked Fluorescein." *Tetrahedron* 72 (7) (2016) 985-91. https://dx.doi.org/10.1016/j.tet.2015.12.068.
85. Rani, B. K. and John, S.A. "A Highly Selective Turn-on Fluorescent Chemosensor for Detecting Zinc Ions in Living Cells Using Symmetrical Pyrene System." *Journal of Photochemistry and Photobiology A: Chemistry* 418 (2021).113372. https://dx.doi.org/10.1016/j.jphotochem.2021.113372.
86. Zhang, P., Xu, X., Cui, Y.F., Wei, X.H., memg, S.J. and Sun,Y.X. "A Highly Sensitive and Selective Bissalamo-Coumarin-Based Fluorescent Chemical Sensor for Cr^{3+}/Al^{3+} Recognition and Continuous Recognition S2." *Journal of Photochemistry and Photobiology A: Chemistry*408 (2021) 113066.https://dx.doi.org/10.1016/j.jphotochem.2020.113066.
87. Li, P. and Xiao, S. "A Highly Sensitive and Selective Sensor Based on Imidazo[1,2- a]Pyridine for Al^{3+}." *Journal of Photochemistry and Photobiology A: Chemistry* 330 (2016) 169-74. https://dx.doi.org/10.1016/j.jphotochem.2016.08.002.
88. Fang, H., Huang, P. C., and Wu, F. Y. "A Highly Sensitive Fluorescent Probe with Different Responses to Cu^{2+} and Zn^{2+}." *Spectrochimica Acta A: Molecular Biomolecular Spectroscopy* 214 (2019) 233-38. https://dx.doi.org/10.1016/j.saa.2019.02.007

89. Fu, Y., Tu, Y., Fan, C., Zheng, C., Liu, G. and Pu,S. "A Highly Sensitive Fluorescent Sensor for $Al^{3+}$and Zn^{2+}Based on a Diarylethene Salicylhydrazide Schiff Base Derivative and Its Bioimaging in Live Cells." *New Journal of Chemistry* 40, (10) (2016) 8579-86. https://dx.doi.org/10.1039/c6nj01458e
90. Wang, H., Zhao, S., Xu, Y., Li, L., Li, B., Pei, M. and Zhang, G. "A New Fluorescent Probe Based on Imidazole[2,1-B]Benzothiazole for Sensitive and Selective Detection of Cu^{2+}." *Journal of Molecular Structure* 1203 (2020) 127384. https://dx.doi.org/10.1016/j.molstruc.2019.127384.
91. Patra, L., Das, S., Gharami, S., Aich, K. and Mondal, T.K. "A New Multi-Analyte Fluorogenic Sensor for Efficient Detection of Al3+and Zn2+Ions Based on Esipt and Chef Features." *New Journal of Chemistry* 42 (23) (2018) 19076-82. https://dx.doi.org/10.1039/c8nj03191f.
92. Dodangeh, M., Gharanjig, K. and Arami, M. "A Novel Ag^{+}Cation Sensor Based on Polyamidoamine Dendrimer Modified with 1,8-Naphthalimide Derivatives." *Spectrochimica Acta A: Molecular and Biomolecular Spectroscopy* 154 (2016) 207-14. https://dx.doi.org/10.1016/j.saa.2015.09.031.
93. Zhao, G., Guo, B., Wei, G., Guang, S., Gu, Z. and Xu, H. "A Novel Dual-Channel Schiff Base Fluorescent Chemo-Sensor for Zn^{2+} and Ca^{2+} Recognition: Synthesis, Mechanism and Application." *Dyes and Pigments* 170 (2019).107614. https://dx.doi.org/10.1016/j.dyepig.2019.107614.
94. Zhu, J., Zhang, Y., Chen, Y., Sun, T., Tang, Y., Huang, Y., Yang, Q., Ma, D., Wang, Y., and Wang,M. "A Schiff Base Fluorescence Probe for Highly Selective Turn-on Recognition of Zn^{2+}." *Tetrahedron Letters* 58 (4) (2017) 365-70. https://dx.doi.org/10.1016/j.tetlet.2016.12.041.
95. Ding, W. H., Cao, W., Zheng, X. J, Ding, W. J, Qiao, J. P. and Jin, L. P. "A Tetrazole-Based Fluorescence "Turn-on" Sensor for Al $^{3+}$ and Zn^{2+} Ions and Its Application in Bioimaging." *Dalton Transactions* 43 (17) (2014) 6429-35. https://dx.doi.org/10.1039/c4dt00009a.

96. Wang, G.Q., Qin, J.C., Fan, L., Li, C.R. and Yang, Z.Y.. "A Turn-on Fluorescent Sensor for Highly Selective Recognition of Mg^{2+} Based on New Schiff's Base Derivative." *Journal of Photochemistry and Photobiology A: Chemistry* 314 (2016) 29-34. https://dx.doi.org/10.1016/j.jphotochem.2015.08.005.
97. Anbu, S., Ravishankaran, R., Guedes da Silva, M. F., Karande, A. A. and Pombeiro, A.J. "Differentially Selective Chemosensor with Fluorescence Off-on Responses on Cu^{2+} and Zn^{2+} Ions in Aqueous Media and Applications in Pyrophosphate Sensing, Live Cell Imaging, and Cytotoxicity." *Inorganic Chemistry* 53 (13) (2014) 6655-64. https://dx.doi.org/10.1021/ic500313m.
98. Alam, R., Mistri, T., Bhowmick, R., Katarkar, A., Chaudhuri, K. and Ali,M. "Esipt Blocked Chef Based Differential Dual Sensor for Zn^{2+} and Al^{3+}in a Pseudo-Aqueous Medium with Intracellular Bio-Imaging Applications and Computational Studies." *RSC Advances* 6 (2) (2016) 1268-78. https://dx.doi.org/10.1039/c5ra18424j.
99. Cheng, X., Yu, Y. Jia, Y. and Duan, L. "Fluorescent Pu Films for Detection and Removal of Hg $^{2+}$, Cr $^{3+}$ and Fe $^{3+}$ Ions." *Materials & Design* 95 (2016) 133-40. https://dx.doi.org/10.1016/j.matdes.2016.01.103.
100.Qin, J. C., Li, T. R., Wang, B. D., Yang, Z. Y. and Fan, L. "Fluorescent Sensor for Selective Detection of Al^{3+} Based on Quinoline-Coumarin Conjugate." *Spectrochimica Acta part A: Molecular Biomolecular Spectroscopy* 133 (2014) 38-43. https://dx.doi.org/10.1016/j.saa.2014.05.033.
101.Piyanuch, P., Watpathomsub, S., Lee, V.S., Nienaber, H.A. and Wanichacheva, N. "Highly Sensitive and Selective Hg^{2+}-Chemosensor Based on Dithia-Cyclic Fluorescein for Optical and Visual-Eye Detections in Aqueous Buffer Solution." *Sensors and Actuators B: Chemical* 224 (2016) 201-08. https://dx.doi.org/10.1016/j.snb.2015.09.131.
102.Cheah, P.W., Heng, M.P., Izati, A., Ng, C.H. and Tan, K.W. "Rhodamine B Conjugate for Rapid Colorimetric and Fluorimetric Detection of Aluminium and Tin Ions and Its Application in Aqueous Media." *Inorganica Chimica Acta* 512 (2020).119901. https://dx.doi.org/10.1016/j.ica.2020.119901.
103.Qin, J.C. and Yang,Z.Y. "Selective Fluorescent Sensor for Al^{3+} Using a Novel Quinoline Derivative in Aqueous Solution." *Synthetic Metals* 209 (2015) 570-76. https://dx.doi.org/10.1016/j.synthmet.2015.09.021.
104.Lee, S. Y., Bok, K.H., Kim, J.A., Kim, S.Y. and Kim, C. "Simultaneous Detection of Cu^{2+} and Cr^{3+} by a Simple Schiff-Base Colorimetric Chemosensor Bearing Nbd (7-Nitrobenzo-2-Oxa-1,3-Diazolyl) and Julolidine Moieties." *Tetrahedron* 72 (35) (2016) 5563-70. https://dx.doi.org/10.1016/j.tet.2016.07.051.
105.Rani, B. K. and John, S. A. "Fluorogenic Mercury Ion Sensor Based on Pyrene-Amino Mercapto Thiadiazole Unit." *Journal of Hazardous Materials* 343 (2018) 98-106. https://dx.doi.org/10.1016/j.jhazmat.2017.09.028.
106.Qin, J.C., Fan, L., Wang, B.D., Yang, Z.Y. and Li, T.R. "The Design of a Simple Fluorescent Chemosensor for Al^{3+}/Zn^{2+}Via Two Different Approaches." *Analytical Methods* 7 (2) (2015) 716-22. https://dx.doi.org/10.1039/c4ay02351j.
107.Zhong, Z., Zhang, D., Li, D., Zheng, G. and Tian, Z. "Turn-on Fluorescence Sensor Based on Naphthalene Anhydride for Hg^{2+}."

Tetrahedron 72 (49) (2016) 8050-54. https://dx.doi.org/10.1016/j.tet.2016.10.033.
108.Choi, Y.W., You, G.R., Lee, J.J. and Kim, C. "Turn-on Fluorescent Chemosensor for Selective Detection of Zn^{2+} in an Aqueous Solution: Experimental and Theoretical Studies." *Inorganic Chemistry Communications* 63 (2016): 35-38. https://dx.doi.org/10.1016/j.inoche.2015.11.012.
109.Ding, Y., Zhao, C., Zhang, P., Chen, Y., Song, W., Liu, G., Liu, Z., Yun, L. and Han, R. "A Novel Quinoline Derivative as Dual Chemosensor for Selective Sensing of Al^{3+} by Fluorescent and Fe^{2+} by Colorimetric Methods." *Journal of Molecular Structure* 1231 (2021) 129965. https://dx.doi.org/10.1016/j.molstruc.2021.129965.
110.Kamel, R.M., El-Sakka, S.S., Bahgat, K., Monir, M.R. and Soliman, M. H. A. "New Turn on Fluorimetric Sensor for Direct Detection of Ultra-Trace Ferric Ions in Industrial Wastewater and Its Application by Test Strips." *Journal of Photochemistry and Photobiology A: Chemistry* 411 (2021).113218. https://dx.doi.org/10.1016/j.jphotochem.2021.113218.